POSITIVE PION - PROTON SCATTERING

IN THE RANGE 10 - 35 MEV.

A thesis presented for the degree of Master of Science in the

University of Liverpool

by

Maria Fidecaro

December 1956

POSITIVE PION - PROTON SCATTERING

IN THE RANGE 10 - 35 MEV.

A Thesis presented for the degree of Master of Science at the

University of Liverpool

by

Maria Fidecaro.

December 1956

The research described in the dissertation was carried out in the Nuclear Physics Research Laboratory.

I am indebted to the International Federation of University Women for the award of a Alice Hamilton fellowship.

My thanks are due to the Prof. H.W.B. Skinner for kind hospitality and to Drs. W.H. Evans, M.H. Alston, G. von Gierke and Mrs. R. Newport and P.R. Williams for invaluable help they gave to me.

Index

Part 1 - THEORETICAL

Part 2 - EXPERIMENTAL

Appendix

A - Corrections to the spectrum assuming that pion decays with a reprojection angle less than 5° are missed during the scanning.

B - Single Coulomb scatterings of pions in hydrogen mistaken for pion decays.

C - Some details of the Liverpool synchrocyclotron.

CAPTION TO THE FIGURES

Part 1 - THEORETICAL

1. Introduction

Since the time pions were first artificially produced, they have been the subject of several theoretical and experimental investigations (1). Some of the established properties of pions are listed in table 1, together with the properties of other elementary particles. However, the nuclear interaction of a pion with a proton or a neutron, a phenomenon which, if one believes to Yukawa original hypothesis (2) is related to the problem of nuclear forces, has not yet been fully understood.

Our knowledge of the pion nucleon interaction is limited to a phenomenological description which seems to be coherent with the ideas of charge symmetry and charge independance, when they are transported from the nuclear forces into the meson physics through the isotopic spin formalism. A complete discussion of the available experimental datas, from the point of view of their interpretation, would be toolong to be reported here (3). We shall discuss only the particular point related to the interaction π+ p, which is the subject of the present experiment. To do that, and at the same time to introduce the problem from a quantum mechanics point of view, we shall develope in the next sections the phenomenological theory of the pion nucleon scattering.

From the point of view of meson theory, only very recently, with the Chew-Low-Wick theory (4), certain features on the π p interaction have been understood. Generally speaking, the meson theory had shown before only a qualitative agreement

with the experiments. Another promising approach has been done with the application to meson waves of the causality relations (5) well known in the field of optics (6). However some discussion is still going on on both these two subjects, which appear to be correlated and we shall not report on them here.

* * *

2. Partial wave analysis

The scattering of a pion by a nucleon is the most simple phenomenon which can be used to study the field of forces generated by a nucleon, in particular to investigate the meson theories. According to the quantum mechanics, the state of two particles is described by a wave function of all the coordinates of both particles satisfying, in non relativistic approximation, the Schrodinger wave equation. Our aim is to acquire a knowledge of the interaction from a study of the relative motion of the two particles. The only experimental information available in this respect is the frequency with which a pion of energy E is scattered in a solid angle $d\Omega$ by a nucleon, i.e. the differential cross section for scattering as a function of energy and angle, $d\sigma / d\Omega$.

In the following we shall refer always to the center of mass system (c.m.s.). A general discussion on collision problems can be found in ref. 7, page 96 and foll. As it is shown there, a two body system in which the interaction is function of the relative distance of the two particles, is described by the same Schrodinger equation which describes the motion, in the field of a fixed scattering center, of a single particle with mass equal to the reduced mass having as linear momentum the common momentum of the two original particles. (r,θ,φ) are the spherical coordinates of this particle, relative to

the fixed scattering center and z the axis from which θ is measured. In this representation r is also the relative distance between pion and nucleon.

We suppose that all the nucleons have spin "parallel" to the z-axis. Because this is not true, we have to average between the cross sections for the two spin orientations, but we shall see that the cross section does not depend on the sign of the z-component of the spin. $\chi^{m_s}_s$ are the eigenfunctions of the S^2 and S_z spin operators, which belong to the eigenvalues $s(s+1)=3/4$ and $m_s = \pm 1/2$.

We had already supposed that the interaction potential V depends on the space coordinates only through r. We add now that it depends also on the spin and charge coordinates of the two particles, and we suppose that it is different from zero only for $r < r^o$.

Let us consider a beam of pions with linear momentum $p = \hbar k$, which moves along the z axis toward a nucleon. Apart from a time factor, the system shall be described by the wave function $\exp(ikz)\chi^{+\frac{1}{2}}_{\frac{1}{2}}$. All the orbital angular momenta are present in this wave, as we shall see later. The direction may be anyone, but the z component must be zero for the particular choice of the z axis.

Since nuclear forces depend on the spin coordinates of the system, we find in the wave representing a system of mesons and nucleons after the interaction both the parallel and the antiparallel orientation for the spin of the nucleons. The probability for the two directions is a priori different. However the total angular momentum J has to be conserved, i.e. if we analyse the wave function in terms of the eigenfunctions of the total angular momentum operators, the presence of the interaction in a region $r < r^o$, can only change by a phase factor the coefficient of each J-eigenfunction [redacted]. In addition, being 1/2 the spin of the nucleon, the conservation of parity requires the conservation of the quantum number ℓ.

Let us call J^m_j the simultaneous eigenfunctions of the total angular momentum operators J^2 and J_z with eigenvalues $j(j+1)$ and m_j respectively; and Y^m_l the simultaneous eigenfunctions of the orbital angular momentum operators L^2 and L_z with eigenvalues $l(l+1)$ and m_l respectively.

For the incoming wave $\exp(ikz)\chi^{+\frac{1}{2}}_{\frac{1}{2}}$ we get at large r :

$$(1)\quad \exp(ikz)\chi^{+\frac{1}{2}}_{\frac{1}{2}} = \sum_{l=0}^{\infty} i^l \sqrt{4\pi(2l+1)}\,\frac{1}{2ikr}\left\{e^{i(kr-l\pi/2)} - e^{-i(kr-l\pi/2)}\right\} Y^0_l \chi^{+\frac{1}{2}}_{\frac{1}{2}}$$

(see Blatt & Weisskopf (8), page 784) i.e. at large r the "incoming" wave looks like a superimposition of "incoming" and "outgoing" waves represented by terms proportional to exp(-ikr) and to exp(ikr) respectively.

By using the rules for vector addition of angular momenta (*) we get :

$$(2)\quad \exp(ikz)\chi^{+\frac{1}{2}}_{\frac{1}{2}} = \sum_{l=0}^{\infty} i^l \sqrt{4\pi(2l+1)}\,\frac{1}{2ikr}\left\{e^{ikr-l\pi/2} - e^{-i(kr-l\pi/2)}\right\} \cdot$$

$$\cdot\left\{\left(\frac{l+1}{2l+1}\right)^{\frac{1}{2}} J^{+\frac{1}{2}}_{l+\frac{1}{2}} - \left(\frac{l}{2l+1}\right)^{\frac{1}{2}} J^{+\frac{1}{2}}_{l-\frac{1}{2}}\right\}$$

For causality reasons the scattering can change only the "outgoing" wave. Let us call $\exp(2i\alpha_{l,j})$ the phase factor for each l and j. The "total" wave must be :

$$(3)\quad \Psi_{tot} = \sum_{l=0}^{\infty} i^l \sqrt{4\pi(2l+1)}\,\frac{1}{2ikr}\left\{e^{i\alpha_{l,l+\frac{1}{2}}} \sin(kr-l\pi/2+\alpha_{l,l+1/2})\left(\frac{l+1}{2l+1}\right)^{1/2} J^{+1/2}_{l+1/2} + \right.$$

$$\left. - e^{i\alpha_{l,l-1/2}} \sin(kr-l\pi/2+\alpha_{l,l-1/2})\left(\frac{l}{2l+1}\right)^{\frac{1}{2}} J^{+\frac{1}{2}}_{l-\frac{1}{2}}\right\}$$

and going back to the eigenfunctions of the orbital momentum operators and of the spin operators

$$(4)\ \Psi_{tot} = \sum_{l=0}^{\infty} i^{l} \sqrt{4\pi(2l+1)}\, \frac{1}{kr} \left\{ \left[e^{i\alpha_{l,l+1/2}} \sin\left(kr - l\pi/2 + \alpha_{l,l+1/2}\right)\left(\frac{l+1}{2l+1}\right) - e^{i\alpha_{l,l-1/2}} \sin\left(kr - l\pi/2 + \alpha_{l,l-1/2}\right)\left(\frac{l}{2l+1}\right) \right] Y_l^0 \chi_{1/2}^{+1/2} + \left[e^{i\alpha_{l,l+1/2}} \sin\left(kr - l\pi/2 + \alpha_{l,l+1/2}\right) - e^{i\alpha_{l,l-1/2}} \sin\left(kr - l\pi/2 + \alpha_{l,l-1/2}\right) \right] \frac{[l(l+1)]^{\frac{1}{2}}}{2l+1} Y_l^1 \chi_{1/2}^{-1/2} \right\}$$

Y_1^m are solutions of the angular part of the Schrodinger equation. The coefficients of Y_1^m are asymptotic solutions of the radial part (**).

The "scattered" wave shall be the difference between the "total" wave and the "incoming" wave.

$$(*)\quad J_{l+\frac{1}{2}}^{+\frac{1}{2}} = \left[\frac{l+1}{2l+1}\right]^{\frac{1}{2}} Y_l^0 \chi_{\frac{1}{2}}^{+\frac{1}{2}} + \left[\frac{l}{2l+1}\right]^{\frac{1}{2}} Y_l^1 \chi_{\frac{1}{2}}^{-\frac{1}{2}}$$

$$J_{l-\frac{1}{2}}^{+\frac{1}{2}} = -\left[\frac{l}{2l+1}\right]^{\frac{1}{2}} Y_l^0 \chi_{\frac{1}{2}}^{+\frac{1}{2}} + \left[\frac{l+1}{2l+1}\right]^{\frac{1}{2}} Y_l^1 \chi_{\frac{1}{2}}^{-\frac{1}{2}}$$

Blatt & Weisskopf (8) page 789.

(**) The general solution of the radial part of the Schrodinger wave equation in a region of zero potential is :

$$(5)\quad a j_l(kr) + b n_l(kr)$$

where :

$$j_l\ (kr) = \sqrt{\pi / 2kr}\quad G_{l+1/2}\ (kr)$$

$$n_l\ (kr) = \sqrt{\pi / 2kr}\quad N_{l+1/2}\ (kr)$$

$G_{l+1/2}$ (kr) is the Bessel function of the first kind, order $\ell+1/2$

$N_{l+1/2}$ (kr) is the Bessel function of the second kind, order $\ell+1/2$.

The asymptotic expressions for j_l and n_l are :

(6) large r ($kr \gg \ell$) $j_l(kr) \rightarrow 1/kr\ \sin(kr-l\pi/2)$
$n_l(kr) \rightarrow 1/kr\ \cos(kr-l\pi/2)$

(7) small r ($kr \lesssim 1$) $j_l(kr) \rightarrow (kr)^l/(2l+1)!!$
$n_l(kr) \rightarrow (2l-1)!!/(kr)^{l+1}$

See L. Schiff (7) page 77.

a and b are determined from the boundary conditions. If the interaction is zero everywhere the solution has to be regular for r=0 and it must be b=0. If the interaction is zero only in the region $r>r^o$, we get $b\neq 0$, so that for large r (5) becomes:

(8) $A/kr\ \sin(kr-l\pi/2 + \alpha)$

The name of phase shift given to α is from here obvious.
a and b are determined by the continuity of the logaritmic derivative of the solution ar $r=r^o$ and by the normalisation condition.

The asymptotic expression for the "scattered" wave is :

$$\Psi_{sc} \sim \sum_{l=0}^{\infty} \sqrt{4\pi(2l+1)}/ikr \left[\left\{ (e^{2i\alpha_{l,l+\frac{1}{2}}} - 1) \frac{l+1}{2l+1} + (e^{2i\alpha_{l,l-\frac{1}{2}}}) \frac{l}{2l+1} \right\} Y_l^0 \chi_{\frac{1}{2}}^{+\frac{1}{2}} \right.$$

$$\left. + \left\{ (e^{2i\alpha_{l,l+\frac{1}{2}}} - 1) - (e^{2i\alpha_{l,l-\frac{1}{2}}}) \right\} \sqrt{\frac{l(l+1)}{2l+1}} \; Y_l^1 \chi_{-\frac{1}{2}}^{-\frac{1}{2}} \right]$$

We assume now that at no too high energies the biggest contribution to the above sum comes from the terms corresponding to l=0 and l=1. This assumption can be justified only to a certain extent, as a complete answer must be left to the experiments (*). We have :

$$Y_0^0 = 1/\sqrt{4\pi} \; ; \; Y_1^0 = \cos\theta \sqrt{3/4\pi} \; ; \; Y_1^1 = -\sin\theta \exp(i\varphi) \sqrt{3/4\pi \cdot 2}$$

$$Y_1^{-1} = + \sqrt{\frac{3}{4\pi \cdot 2}} (\sin\theta) \; e^{-i\varphi}$$

If we call :

$$a_s = \exp(2i\alpha_{0\frac{1}{2}}) - 1 \tag{9}$$

$$a_{P_1} = \exp(2i\alpha_{1\frac{1}{2}}) - 1$$

$$a_{P3} = \exp(2i\alpha_{1\,3/2}) - 1$$

we finally obtain for the amplitude of the scattered wave :

$$S = \exp(ikr)/2ikr \left\{ \chi_{\frac{1}{2}}^{+\frac{1}{2}} \left[a_s + \cos\theta (2a_{P3} + a_{P1}) \right] \chi_{\frac{1}{2}}^{-\frac{1}{2}} \sin\theta e^{i\varphi} \left[a_{P3} - a_{P1} \right] \right\} \tag{10}$$

The plane wave $\exp(ikz)\chi_{\frac{1}{2}}^{+\frac{1}{2}}$ represents a density of one meson and one nucleon per unit volume, and a flow of v mesons across the scatterer per unit area and unit time. The number of mesons in the scattered wave crossing an element of area ds at the point (r,θ,φ) is $v \cdot ds \cdot |S|^2$ per unit time, and $|S|^2 r^2 v$ per unit time and unit solid angle ($d\Omega = ds/r^2$).

The cross section shall be :

$$(11)\quad d\sigma/d\Omega = \frac{1}{4k^2}\left\{|a_s+\cos\theta(2a_{P3}+a_{P1})|^2+|\sin\theta(a_{P3}-a_{P1})|^2\right\}$$

Here we have used the orthogonality of the spin eigenfunctions.

The first term in (11) is called "no-spin flip" term, the second one "spin flip".

If $a_{P3} = a_{P1}$, i.e. if the nuclear forces are spin independent, we obtain the standards result of the scattering theory (see for example N.F. Mott and H.S.W. Massey (10), chapter II and sparsim.

The relativistic expression for $d\sigma/d\Omega$ is obtained from (11) when the relativistic formula is used to calculate k. To show this, we have to consider the nucleons as infinitely heavy and use the Klein-Gordon equation, which is valid for particles of spin zero.

As it is showed in the foot-note, the interaction is related to the cross-section through the phase-shifts. It is whorth noting that it is possible to obtain the phase-shifts from a potential, but the viceversa is not true.

(*) According to Hofstadter & Mc Allister (49). $\lambda^0 \sim 0.7\ \hbar/\mu c$. Now a classical particle is not scattered if its trajectory does not enter the interaction region $r<r^0$. By the correspondance principle we expect that only waves with angular momenta $l\hbar$ not much bigger than $\hbar k r^0$ (that is with l not much bigger than η) contribute to the scattering amplitude. Moreover, in the vicinity of r^0, if $kr^0 \leq 1$ (that is $\eta \leq 1$) we may use (5) and (7) to write the solution of the Schrodinger equation for $r>r^0$. If $\rho(E)$ is the logarithmic derivative of the solution computed for $r=r^0$, matching at r^0 we get :

$$tg\alpha = \left[\frac{(l+1)\rho(E)-r^0}{l\rho(E)+r^0}\right] \times \frac{(kr^0)^{2l+1}}{(2l+1)!!(2l-1)!!}$$

For small values of E, ρ (E) can be substituted by its value at zero energy so that

$$tg\alpha \sim \alpha \simeq const \frac{(kr^{0})^{2\ell+1}}{(2\ell+1)!!(2\ell-1)!!}$$

The denominator grows rapidly as ℓ increases, which confirms the small importance of high ℓ waves.

(See E. Fermi (9), page 40 and foll.)

* * *

3. The isotopic spin

The cross section for pion nucleon scattering is different according that the pion is positive, negative or neutral, and the nucleon is a neutron or a proton. As we have seen above, these cross sections can be written in terms of phase shifts for each charge combination of the pion nucleon system. Let us now introduce the isospin notation.

According to the original suggestion by Heisenberg (11) we may consider protons and neutrons as different states of the same particle and label the two eigenstates with a two value coordinate. The operators which operate on such a coordinate obey the same commutation rules as for ordinary angular momenta. Thus we can assigne to a nucleon a sort of spin defined in a fictitious space, the charge space. The quantum numbers are $\tau = 1/2$ and $\tau_3 = \pm 1/2$ (+ for proton, - for neutron). The charge of the nucleon is related to the "z" component τ_3 in the following way :

$$Q = \tau_3 + 1/2$$

We introduce now the physical principle of charge independence of nuclear forces, which means that the forces between two protons ot two neutrons or also between a proton and a neutron, are the same. It is possible to show from this assumption that the total isospin of a system of particles is time invariant. (See for example, ref. 9, page 21 and foll.)
This, and a consideration of the Yukawa reactions

$$n \rightarrow \pi^- + p \quad \text{etc.}$$

suggest that pions of different charge are conveniently represented by an isospin corresponding to quantum numbers $\tau = 1$ and $\tau_3 = +1, 0, -1$, for positive, neutral and negative pions respectively. In this case the charge of the pion is equal to the "z" component τ_3. The usual rules for addition of angular momenta give as possible values for the total isospin of a system of a meson and a nucleon 3/2 and 1/2.

Going back to the π p scattering it is possible to show, with a formalism similar to that adopted before for the angular momenta in the ordinary space, that there are only two phase shifts for each j and ℓ, one for each of the two states of isotopic spin 3/2 and 1/2. We shall indicate the procedure very briefly.

Let us call $I^{T}_{T_3}$ the eigenfunction of the "total" isospin with eigenvalues T and T_3. The eigenfunctions for a pion nucleon system are :

$T = 3/2$	$T = 1/2$
$I^{+3/2}_{3/2} = (p+)$	
$I^{+1/2}_{3/2} = \sqrt{2/3}\ (po) + \sqrt{1/3}\ (n+)$	$I^{+1/2}_{1/2} = -\sqrt{1/3}\ (po) + \sqrt{2/3}\ (n+)$
$I^{-1/2}_{3/2} = \sqrt{2/3}\ (no) + \sqrt{1/3}\ (p-)$	$I^{-1/2}_{1/2} = \sqrt{1/3}\ (no) + \sqrt{2/3}\ (p-)$
$I^{-3/2}_{3/2} = (n-)$	

(12)

where (p+) is the eigenfunction for a system of a proton and a π^+, (po) a proton and a π^o, and so on. The numerical coefficients are the Clebtsch-Gordan coefficients.

Let us call S_3 and S_1 the scattering amplitudes corresponding to scattering in the different isospin states 3/2 and 1/2. We have :

$$(13)\quad \chi^{+\frac{1}{2}}_{\frac{1}{2}} \exp(ikz) \cdot I^{(\pm\frac{1}{2})}_{\frac{1}{2}} \rightarrow S_1 \cdot I^{\pm\frac{1}{2}}_{\frac{1}{2}}$$

$$\chi^{+\frac{1}{2}}_{\frac{1}{2}} \exp(ikz) \cdot I^{(3/2)}_{3/2} \rightarrow S_3 \cdot I^{(3/2)}_{3/2}$$

From (12) we get :

$$(14)\quad (p+) = I^{3/2}_{3/2}$$

$$(no) = \sqrt{2/3}\, I^{+\frac{1}{2}}_{3/2} + \sqrt{1/3}\, I^{+\frac{1}{2}}_{\frac{1}{2}}$$

$$(p-) = \sqrt{1/3}\, I^{-\frac{1}{2}}_{3/2} - \sqrt{2/3}\, I^{-\frac{1}{2}}_{\frac{1}{2}}$$

$$(n-) = I^{-3/2}_{3/2}$$

and so on.

It follows that :

$$(15)\quad \chi^{+\frac{1}{2}}_{\frac{1}{2}} \cdot (p+) \cdot \exp(ikz) \rightarrow S_3\, I^{3/2}_{3/2} = S_3\,(p+)$$

$$\chi^{+\frac{1}{2}}_{\frac{1}{2}} \cdot (p-) \cdot \exp(ikz) \rightarrow \sqrt{1/3}\, S_3\, I^{-\frac{1}{2}}_{3/2} - \sqrt{2/3}\, S_1\, I^{-\frac{1}{2}}_{\frac{1}{2}} =$$

$$= (no)\, \tfrac{1}{3}\cdot\sqrt{2} \cdot (S_3 - S_1) + (p-)\, \sqrt{1/3}\, (S_3 + 2S_1)$$

In the (p-) scattering, the amplitude $1/3\,(S_3 + 2S_1)$ describes the elastic scattering of negative pions by protons and

the amplitude $\sqrt{2/3}\ (S_3 - S_1)$ describes the charge exchange scattering.

Adopting a Fermi notation, the S wave phase shift ($\ell = 0$) with isospin 3/2 and 1/2 will be indicated by α_3 and α_1 respectively. The phase shifts for P waves ($\ell = 1$) will be indicated by α_{33} α_{31} α_{13} α_{11}, where the first index is twice the isospin and the second index is twice the angular momentum.

Let us put :

$$(16) \qquad e_3 = \exp(2i\alpha_3) - 1$$

and so on.

From (10) and (16) we get :

$$(17) \qquad S_3 = \text{expikr}/2\text{ikr}\left\{\left[e_3+(2e_{33}+e_{31})\cos\theta\right]\chi^{+\frac{1}{2}}_{\frac{1}{2}} + (e_{31}-e_{33})\sin\theta e^{i\varphi}\chi^{-\frac{1}{2}}_{\frac{1}{2}}\right\}$$

$$S_1 = \text{expikr}/2\text{ikr}\left\{\left[e_1+(2e_{13}+e_{11})\cos\theta\right]\chi^{+\frac{1}{2}}_{\frac{1}{2}} + (e_{11}-e_{13})\sin\theta e^{i\varphi}\chi^{-\frac{1}{2}}_{\frac{1}{2}}\right\}$$

and :

$$(18) \qquad \frac{d6}{d\Omega}(p+,p+) = \left\{\left|e_3+(2e_{33}+e_{31})\cos\theta\right|^2+\left|e_{31}-e_{33}\right|^2\sin^2\theta\right\}1/4k^2$$

$$(19) \qquad \frac{d6}{d\Omega}(p-,no) = \left\{\left|e_3-e_1+\left[2(e_{33}-e_{13})+e_{31}-e_{11}\right]\cos\theta\right|^2+\left|(e31-e_{33})\right.\right.$$
$$\left.\left.-(e_{11}-e_{13})\right|^2\sin^2\theta\right\} \cdot \tfrac{1}{4}k^2 \cdot 2/9$$

$$(20)\quad \frac{d\sigma}{d\Omega}(p-,p-)=\Big\{\Big|e_{31}+2e_1+\big[2e_{33}+e_{31}+2(2e_{13}+e_{11})\big]\cos\theta\Big|^2 + \Big|e_{31}-e_{33}+2(e_{11}-e_{33})\Big|^2\sin^2\theta\Big\}\cdot\frac{1}{4k^2}\cdot 1/9$$

and so on.

Thus, if we consider only S and P waves, the cross sections we can measure in pion nucleon scattering are completely defined by a set of six constants (functions of the energy).

* * *

4. The Coulomb potential.

To take into account the Coulomb forces, which are long range forces, we shall consider them negligible inside the region (of radius of the order of meson Compton wave lenght; see page 13) in which nuclear forces act, and use the appropriate Coulomb wave function outside. It turns out that the scattering amplitude for not too low energy can be written, to quite a good approximation, as a sum of the nuclear amplitude in term of phase shifts and the Coulomb amplitude in the Born approximation. In this approximation the Coulomb amplitude is given by :

$$(21)\quad f^{(nf)}(\theta) = \frac{-}{+}\frac{e^2/h}{2kv\,\sin^2\theta/2} \qquad \text{no spin flip.}$$

$$(22)\quad f^{(f)}(\theta) = \text{zero} \qquad \text{spin flip.}$$

The upper and lower signs in $f^{(nf)}(\theta)$ are valid respectively for (p+) and (p-) scattering. This expression, suggested by

F. Solmitz (12) is not relativistic.

Van Hove (13) has also investigated the Coulomb contribution to the nuclear scattering of pions. (See also ref. (10), page 48). We shall not report his results as they are much more complicated and turn out into the Solmitz formula when $\alpha = e^2/\hbar v$ is sufficiently small ($\lesssim 10^{-2}$). α (10 MeV) = 2 10^{-2}, α (5 MeV) = 2.8 10^{-2}. v is here as well in (21) the relative velocity of the pion to the nucleon.

There has been some discussion about the relativistic extension of (21) and (22). See for example the Solmitz paper.

The Solmitz relativistic formula is :

$$(23)\quad f^{(nf)} = \mp \frac{e^2}{2\hbar k(v_\pi + v_p)\sin^2\theta/2}\left[1+\frac{v_\pi v_p}{2c^2}(1+\cos\theta)+\text{smaller terms}\right]$$

$$(24)\quad f^{(f)} = \pm \frac{e^2}{2\hbar k(v\pi+v_p)\sin^2\theta/2}\left[\mu_p \cdot \frac{v_\pi v_p}{2c^2} + \text{smaller terms}\right]$$

where v_π, v_p are the pion and proton velocities in c.m.s. c is the velocity of the light, μ_p is the magnetic moment of the proton in nuclear magnetons.

The Van Hove's relativistic formula in the above mentioned approximation ($\alpha \lesssim 10^{-2}$) is :

$$(25)\quad f^{(fn)} = \mp \frac{e^2}{2\hbar k v \sin^2\theta/2}$$

$$(26)\quad f^{(f)} = \text{zero.}$$

For small angles of scattering v_p is always small, so that the two expressions, by Solmitz and by Van Hove are identical when

the Coulomb correction could be important.

* * *

5. Some experimental results.

The scattering $\pi - p$ has been extensively studied in several experiments (for low energy experiments $\lesssim 40$ MeV see part II, section 2. For higher energy, to which we do not refer particularly, see ref. 1) Two interesting features have been discovered. First, it has been confirmed that it is possible to interpret the results in terms of 6 phase shifts only (14), as suggested by the charge independence hypothesis developed in section 3. Second, the $\pi - p$ scattering cross sections have a peak at about 190 MeV kinetic energy of the π -meson, which has been interpreted as a resonance in the state with $J = 3/2$, $T = 3/2$. We shall not discuss these points as we are here mainly interested in S wave scattering, because of the lack of direct experimental information on one side, and the connection with experiments on photoproduction of mesons (see section 6) on the other side.

The connection between π-p forces and S wave phase shifts has been the subject of considerable discussion. S wave scattering becomes predominant at low energy ($\lesssim$40 MeV). In this region the dependence of the phase shift on the momentum can be derived from the assumption that the π- p interaction is due to short range forces (see Gell-Mann & Watson (36) page 221). In this case we should expect at very low energy the S wave phase shifts α_3 and α_1 to be linear functions of the momentum of the incoming pion (see note at page 13). The experimental results available until 1955 have been analysed by J. Orear (15) (16) from this point of view. According to Orear :

(27) $\alpha_3 = -0.11\eta$

$\alpha_1 = +0.16\eta$

where η is the momentum of π meson in c.m.s. in μc units.

Nowdays a linear dependence like the one suggested by Orear in (27) is generally accepted at least at very low energy, because of new experimental information, including the results of the present work, an experiment by D. Stork and S.L. Whetstone and other experiments.

(See Part II, section 9 and fig. 15).

This interpretation is quite simple. However people were brought to more complicated arguments, mainly because of the uncertainty of the experimental datas.

In fact, from the previous experimental indications reported at the Rochester Conference 1953 (17 a), it appeared that α_3 could be positive at very low energy and negative at higher energy. As a consequence, Bethe and Noyes discussed the possibility, reported at the Rochester Conference 1954 (16 b), of a Jastrow type potential [redacted], [redacted] which had been suggested by Marshak (19). Such a potential would cause α_3 to depart violently from a linear dependence at about $\eta = 0.3$, and in some proposals α_3 would change sign at about $\eta = 0.5$. Bethe and De Hoffmann looked also at the possibility that $\alpha_3 = 0$ up to $\eta = 0.3$.

FIG. 1

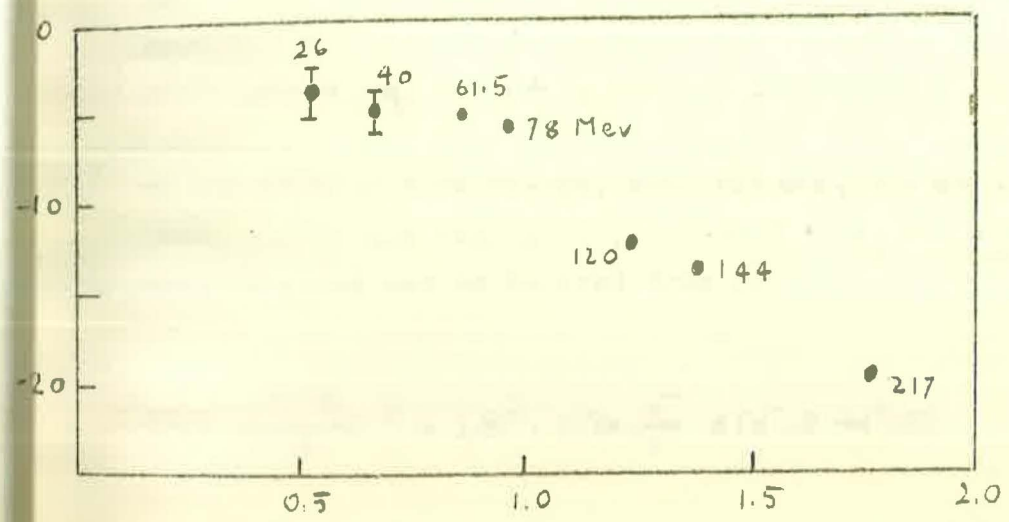

from Bethe de Hoffman
Mesons vol II pag 107

After the Orear papers, at the 5th Rochester Conference (17 e) there was some discussion whether α_3 was changing its slope at some low energy or not, as the experimental points were like those reported in fig. 1. In the Orear analysis more weight had been given to the scattering experiments at not too low energy, rather than to the photoproduction experiments.

* * *

6. Connection of S phase shifts with photoproduction experiments

As we have mentionned in the preceding section there exists a relation between the photoproduction of mesons and the phase difference $\alpha_3-\alpha_1$, for $\eta \to 0$, through the Panofsky ratio (15)(21).

At essentially zero energy, when $\sin\alpha\sim\alpha$, $\cos\alpha\sim 1$, and the P phase shifts are negligible, compared to α_3 and α_1, the following relation can be derived from (19) :

$$(28)\quad \left(\frac{\alpha_3-\alpha_1}{\eta}\right)^2 = 1/\hbar^2 \cdot 9/8\pi \cdot \frac{v^-}{v^o}\ \sigma(\pi^- + P \to \pi^o + N)$$

Here we have taken into account the mass difference between π^- and π^o which had not been included in (19), therefore $v^-/v^o \neq 1$. We obtain :

$$(29)\quad \lim_{\eta\to o}\left(\frac{\alpha_3-\alpha_1}{\eta}\right)^2 = 1/\hbar^2\ 9/8\pi.1/v^o \lim_{\eta\to o} v^- \cdot \sigma(\pi^- + P \to \pi^o + N) =$$

$$= 1/\hbar^2\ 9/8\pi \cdot 1/v^o \cdot P \cdot \lim_{\eta\to o} v^- \cdot \sigma(\pi^- + P \to \gamma + N)$$

Where P is the Panofsky ratio :

$$P = \lim_{\eta\to o} \frac{\sigma(\pi^- + P \to \pi^o + N)}{\sigma(\pi^- + P \to \gamma + N)}$$

By detailed balance :

$$(30) \quad v^- \cdot \sigma(\pi^- + P \rightarrow \gamma + N) = 2 \left(\frac{P\gamma}{P_-}\right)^2 \sigma(\gamma + N \rightarrow \pi^- + P)\, v^-$$

p_γ and p_- are the momenta of the γ and the pion in c.m.s.

According to Bernardini and Goldwasser (22) the S wave contribution to the photoproduction is :

$$(31) \quad \sigma_S(\gamma + P \rightarrow \pi^+ + N) = 1.55\ 10^{-28} \eta \ cm^2$$

Therefore :

$$(32) \quad \lim_{\eta \to o} v^- .2.(P\gamma/P_-)^2\ \sigma(\gamma + N \rightarrow \pi^- + P) = \lim_{\eta \to o} r.1.55\ 10^{-28} \times \eta .2. \frac{P\gamma^2}{\eta^2} (\mu c)^2$$

where : $r = \dfrac{\sigma(\gamma + N \rightarrow \pi^- + P)}{\sigma(\gamma + P \rightarrow \pi^+ + N)}$ and $r^o = \lim_{\eta \to o} r$

Substituting in (29) we get :

$$(33) \quad \lim_{\eta \to o} \left(\frac{\alpha_3 - \alpha_1}{\eta}\right)^2 = \left(\frac{\mu c}{\hbar}\right)^2 .9/8\pi .1/v^o\ P.r^o.1.55\ 10^{-28}.2 \left(\frac{P\gamma c}{\mu c\ 2\hbar}\right)^2 \lim_{\eta \to o} \frac{v^-}{\eta}$$

v_o = velocity of π^o in the Panofsky effect = 0.20 c.

Finally we have :

$$(34) \quad \lim_{\eta \to o} \left(\frac{\alpha_3 - \alpha_1}{\eta}\right) = 0.156\ (P.r^o)^{\frac{1}{2}}$$

r^o (r at threshold) is evaluated from the experimental datas on π^- and π^+ photoproduction in deuterium.

According to Orear (15), we should correct the ratio r^o obtained from deuterium experiments because of a Coulomb effect and increase it by 10 - 30 % to get the true ratio for free nucleons.

According to Benevento et al (23) a rough calculation by Chew and Low (not published) gives a correction of 7 % at 185 MeV photon energy in the laboratory system, 4 % at 205 MeV and 3 % at 225 MeV. Following Benevento et al. we shall neglect this correction.

Therefore we assume for r^o the value obtained by Benevento et al.

$$r^o = 1.87 \pm 0.13$$

P was first evaluated by Panofsky et al. (24) and more recently by Cassels et al. and (25) Kuhner et al. (26)

Panofsky et al.	(1951)	P =	0.94 ± 0.20
Cassels et al.	(1956)		1.50 ± 0.11
Kuhner et al.	(1956)		$1.49 \pm$

Taking Panofsky result we get :

(35) $\alpha_1 - \alpha_3 = 0.206\,\eta$

to be compared with Orear's :

(36) $\alpha_1 - \alpha_3 = 0.27\,\eta$

If we take for P the most recent value 1.50 we get :

$$\alpha_1 - \alpha_3 = 0.26\,\eta$$

The agreement with Orear is much better. Moreover the errors in both the determinations of $\alpha_1 - \alpha_3$ are smaller - See note at pag. 78

We have to mention that before the new measurement of the Panofsky ratio, Noyes (27) tried to reconcile the phase difference $\alpha_3-\alpha_1$ obtained from the Orear phase shifts with (35), assuming non conservation of isotopic spin. Noyes used a charge independent potential for the π-nucleon interaction and included only those isotopic spin dependent terms already required by the experiment : the π^-,π^o mass difference and n-p mass difference, the Coulomb interaction and a radiative capture interaction adjusted to fit the experimental Pahofsky ratio. He says that if $|\alpha_3-\alpha_1|/\eta = 0.27$ as calculated from the scattering experiments, $|\alpha_3-\alpha_1|/\eta = 0.24$ as calculated from the Panofsky effect ($P = 0.94 \pm 0.20$). This evaluation gives only an indication for the direction of the correction, because Noyes used a model for the S wave interaction consisting in a repulsive core surrounded by a attractive potential at longer range, of the kind suggested by Marshak.

We know now that for causality reason this kind of potential has to be refused, as well any strange behaviour of α_3, as suggested from the quite precise knowledge of scattering datas at higher energy (17d).

* * *

Part 2 - EXPERIMENT

1. Aim of the work

The present experiment was planned to determine a more precise value for α_3 at energies $\sim$20 MeV. The arguments in support of this π^+ p scattering experiment have been reported in part 1, sect. 5 & 6.

The experiment consists in a measurement of the total cross section for π^+ p scattering. Using the results of section (2) and (3) and taking into account the Coulomb interaction, section (4), we have at very low energy(*) :

$$(37)\quad d\sigma/d\Omega\ (p\pi^+ \to p\pi^+) = \tfrac{1}{4}k^2 \left\{ \left| \alpha_1 + \cos\theta(2\alpha_{33}+\alpha_{31}) - \right. \right.$$

$$\left. \left. - \frac{e^2}{\hbar} \frac{1}{(v_\pi + v_\rho)\sin^2\theta} \right|^2 + \left| (\alpha_{33}-\alpha_{31})\sin\theta \right|^2 \right\}$$

and for integral cross section with $\theta > \theta_o$ (the lower limit having been introduced to attenuate the Coulomb contribution) :

$$(38)\quad \sigma_{>\theta_o}\ (p\pi^+ \to p\pi^+) = \tfrac{1}{2}\pi k^2 \left\{ \left[(1+\cos\theta_o)(a'^2+c'^2) - (1-\cos^2\theta^o)a'b' + \right.\right.$$

$$\left.\left. + 1/3(1+\cos^3\theta o)(b'^2-c'^2) \right] + \left[C_1\alpha^2 - 2C_2\alpha(a'+b') + 2C_3\,\alpha\, b' \right] \right\}$$

(*) We have assumed $\cos\alpha \sim 1-\sin\alpha \sim \alpha$, because the phase-shifts approache zero as the energy is decreased - See foot-note page 13.

$$a' = \alpha_3 \qquad b' = 2\alpha_{33} + \alpha_{31} \qquad c' = \alpha_{33} - \alpha_{31}$$

$$C_1 = \frac{1}{1 - \cos\theta_o} - 1/2 \qquad C_2 = \ln 2 - \ln (1-\cos\theta_o)$$

$$C = 1 + \cos\theta_o \qquad \alpha = e^2 / (\hbar v) \qquad v = \text{velocity of the meson (lab).}$$

There are some experimental indications that $\alpha_{31} = 0$, α_{33} is well known, (see ref. 1), and at our energies it is comparable with α_3, so that α_3 itself can be determined. Therefore the principle of this experiment rests on the fact that the s-wave scattering is not masked by the p-wave. Obviously the interpretation of the experiment is easier with π^+ rather with π^-, because only the isotopic spin 3/2 has to be considered.

* * *

2. Previous experiments

The following is a list of the experiments connected with the problem of low energy $\pi^{\pm}$ p scattering. (28 ÷ 41)

1) A. Roberts and J. Tinlot, Phys.Rev. 90, 951, 1953.

Charge exchange scattering of negative and positive pions in hydrogen and deuterium. The energy was 34^{+7}_{-8} MeV. They found for charge exchange scattering in hydrogen total cross section 5.0 mbarns for π^- at 34 MeV, and zero for π^+ of the same energy. The total cross-section in deuterium was about 1/3 the cross-section for hydrogen with mesons of both signs.

2) A. Roberts and J. Tinlot, Phys.Rev. 95, 137, 1954.
Angular distribution of charge exchange scattering in hydrogen for 40^{+3}_{-6} MeV negative pions. They found :

$$d\sigma/d\Omega = (0.45 \pm 0.07) - (0.98 \pm 0.13)\cos\theta + (0.54 \pm 0.21)\cos^2\theta$$

corresponding to a total cross-section of 7.9 ± 1.8 mbarns.
In 1) as well in 2) scintillation counters and a subtraction method CH_2 - C and D_2O - H_2O, were used.

3) a: C.E. Angell and J.P. Perry, Phys.Rev. 91, 1283, 1953, angular distribution in π^+ p elastic scattering at 40 MeV.

b: C.E. Angell and J.P. Perry, Phys.Rev. 92, 835, 1953, total cross-section of positive and negative pions in hydrogen at 37 MeV.

c: S.W. Barnes, C.E. Angell, J.P. Perry, D. Millar, J. Ring, D. Nelson, Phys.Rev. 92, 1327, 1953, negative pions elastic scattering at 45° and 40 MeV.
These experiments were all done with counters and subtraction method.

4) S.L. Leonard and D.H. Stork, Phys.Rev. 93, 568, 1954.
Total cross-section for $33 \pm 4,5$ MeV positive pions in hydrogen target. σ tot for scattering angle larger than 35° was 6.4 ± 1.2 mbarns.

5) J. Spry, Phys.Rev. 95, 1295, 1954.
Total cross-section for charge exchange scattering of negative pions in hydrogen, with scintillations counters and subtraction method. He found :

at 42 ± 2 MeV	$\sigma = 6.2 \pm 1.2$ mbarns
30 ± 2	5.7 ± 0.9
20 ± 2	5.0 ± 0.8

6) J. Orear, W. Slater, J.J. Lord, S.L. Eilenberg and A.B. Weaver, Phys.Rev. 96, 174, 1954.

Elastic scattering of 26 ± 2 MeV negative pions by hydrogen with emulsion tecnique. The cross-section for scattering angles between 50° and 180° was 1.15 ± 0.6 mbarns evaluated on 5 events.

7) M.C. Rinehart, K.C. Rogers and L.M. Ledermann, Phys.Rev. 100, 883, 1955.

Elastic scattering of negative pions between 2.5 and 30 MeV with a diffusion cloud chamber. 26 events were found.

8) J. Orear, Phys.Rev. 98, 239, 1955 A and Proc. of 5° Rochester Conference.

Elastic scattering of 23 MeV positive pions in hydrogen with emusion tecnique. The cross-section evaluated on 8 events was 5.5 mbarns.

9) S. Wheastone and D. Stork, Phys.Rev. 102, 251, 1956.

Elastic scattering of 21.5 ± 3.5 MeV positive pions by hydrogen, with a liquid hydrogen target and emulsion detector.

10) S.W. Barnes, Proc. of 6° Rochester Conference.

Differential cross-section of 40 ± 4 MeV positive and negative pions, with scintillation counters and liquid hydrogen target. He found :

$$d\sigma/d\Omega = \begin{cases} 0.32 \pm 0.04 \\ 0.70 \pm 0.08 \end{cases} \text{mbarns sterad}^{-1} \quad \begin{matrix} \pi^+ \\ \pi^- \end{matrix} \Big\} \text{ at } 44^\circ$$

$$\begin{cases} 0.72 \pm 0.035 \\ 0.106 \pm 0.038 \end{cases} \quad \begin{matrix} \pi^+ \\ \pi^- \end{matrix} \Big\} \text{ at } 100^\circ$$

11) D.E. Nagle, R.H. Hildebrand, R.G. Plano, R.S.I. 27, 283, 1956, and Proc. Geneva Conference.

Elastic Scattering of negative pions with a liquid hydrogen bubble chamber. The energy was between 10 and 30 MeV.

12) Some results can also be obtained from mesic atoms experiments. See e.g. M. Camac, A.D. Mc Guire, J.B. Platt and H.J. Schulte, Phys.Rev. 99, 897, 1955. But as in the words of other authors, "the agreement (with scattering experiments)... may be fortuitous... because of the extrapolation and oversemplification involved in the theoretical estimate" (M.Stearns, M.B. Stearns, S. Debenedetti and L. Leipuner, Phys.Rev. 97, 240, 1955).

We have reported the cross-section only in the case that the authors have evaluated it. The results of the measurements concerning only α_3 are summarized in fig. 15, together with the higher energy experiments which are not mentioned above.

* * *

3. The present experiment

We have considered three different techniques which could have been used for this experiment.

1) counter technique with a liquid hydrogen target or a polythene target, if a subtraction method CH_2-C is used. In principle it is possible to get good statistics but unfortunately the angular resolution is poor because of the finite size of the counters and the target. This disadvantage is common to scattering experiments at any energy. At very low energies there are other drawbacks, which cannot be easily avoided with counters. In fact, the probability for π-μ decays in flight increases when the energy decreases, and it is impossible, without special precautions, to recognize a scattering event from a $\pi \rightarrow \mu$

decay. A part from that, the pions must have sufficient energy to escape from the target and reach the counters. The effects are more troublesome when the primary spectrum of the pions is broad. In practice they set a lower limit at 30-40 MeV to the range of energy in which it is possible to use counters for scattering experiments.

2) Nuclear emulsions, It is possible to use two methods. The first method is based on the possibility of recognizing scattering events from the kinematics of the interactions. It is a slow and tedious method but can be used if sufficient man power for the scanning is available. The second method consists in putting emulsions as a detector in the vicinity of a liquid hydrogen target. This method allows for better statistics, but cannot be used for very low energies because scattered pions must have sufficient energy to get out from the target and to be recorded in the emulsion. In addition it is not possible to "see" the events and reconstruct completely their kinematics.

3) Cloud chamber or bubble chamber technique. In a certain way a diffusion cloud chamber filled with hydrogen and operated in a magnetic field is an ideal instrument for elastic π-p scattering experiments at low energy. The fact that the events are seen is a noteworthy advantage as it allows the most complete information on the interactions, leaving little doubt as to the interpretation of the events. This point is very important when rare events have to be selected. On the other hand it is not easy accumulate good statistics, as with counters experiments.

One could also consider, of course, the possible use of a high pressure expansion chamber, but this technique is still in a development stage, because of the long recycling time and the larger distorsions.

A bubble chamber has advantages similar to a diffusion chamber. However, because of the higher density of liquid hydrogen -0.07

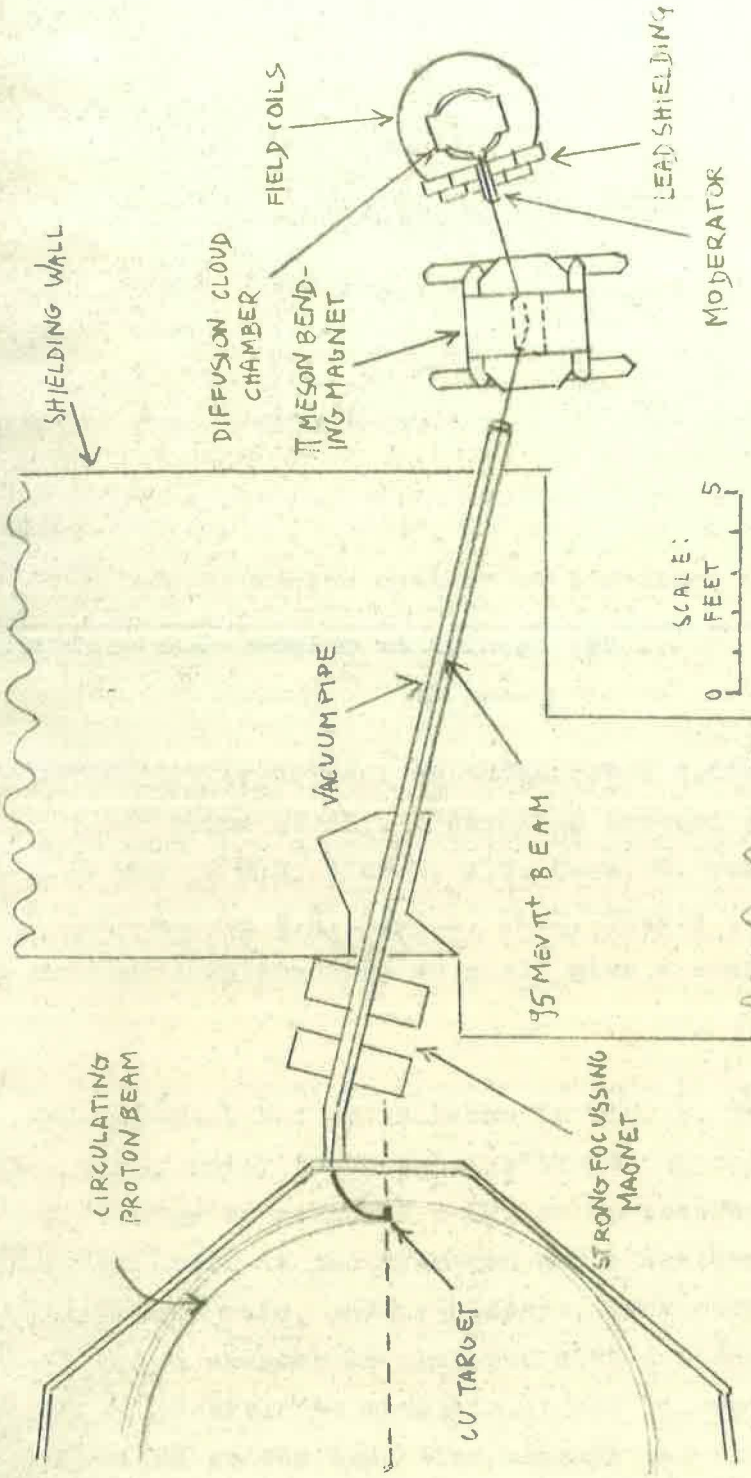
SHIELDING WALL
DIFFUSION CLOUD CHAMBER
FIELD COILS
π MESON BENDING MAGNET
LEAD SHIELDING
MODERATOR
VACUUM PIPE
SCALE: FEET 0 5
95 MeV π+ BEAM
CIRCULATING PROTON BEAM
CU TARGET
STRONG FOCUSSING MAGNET

FIG. 1

gr. cm^{-3} - in comparison to the pressurized hydrogen of a cloud chamber, the probability of producing interactions is much larger, so that it is possible to get better statistics-

The following table is a short comparison between a diffusion chamber and a bubble chamber which are being used at present for low energy π-p scattering experiments :

- 27 -

	Diff. Chamber (1)	Bubble Chamber (2)
Recycling time ...	20 sec.	2 sec.
Hydrogen traversed by each track	0.1 gr cm^{-2}	0.6 gr cm^{-2}
Sensitive time ...	continuous	0.2 sec.

1) 18" 25 atm diffusion chamber at Liverpool (42)(43).

2) 10 cm bubble chamber at Chicago (39).

In the present experiment we have used a diffusion chamber built by W. Evans et al.. A detailed account on the chamber can be found in M.H. Alston, A.V. Crew, G. von Gierke, W.H. Evans (42) and in M.H. Alston, Ph.D. Thesis (43). However, for sake of completeness, we shall give a short description in sec. 5.

The experimental set up is shown in fig. 2. The 95 MeV positive pions enter the chamber after being moderated to the desired energy by means of a CH_2 or Cu absorber. Two kind of events may occur in the hydrogen gas : scattering events, which are very rare, and $\pi - \mu$ decays, much more frequently. The diffusion chamber is operated with a magnetic field, so that it is possible to reconstruct the kinematic of both kind of events and at the same time measure the spectrum of the beam.

We have taken advantage of the presence of the $\pi \rightarrow \mu$ decays to monitor the incident pion beam, as we shall show in section 7.

Before reporting the results we shall discuss in the next sections the low energy beams, the Liverpool diffusion chamber and its operating conditions, the reprojection system, and details of the analysis of the photographs.

* * *

4. Consideration on low energy pion beams

The ideal thing would be to obtain a monoenergetic beam of pions in the 20-30 MeV range. The lack of a monoenergetic beam results in increased work to scan the pictures, and in a larger uncertainty in the determination of the energy at which the experiment is done. In practice it is necessary to find a compromise between the amount of development work needed to make such a monoenergetic beam, and the above mentioned disadvantage.

The problem of a low energy beam has been resolved in different ways in the various laboratories, according to the characteristics of the machines, the general background, the intensity, energy, and degree of monochromaticity required.

The main characteristics of a beam of particles are :

a) The monochromaticity $\Delta E/E$.
b) The available intensity in the energy range ΔE.
c) Geometrical characteristic of the beam. For a diffusion chamber it is necessary to have a parallel beam, with a large separation of the tracks.
d) Contamination from other particles. The contamination increases when the energy of the pions decreases.

It seems that people have considered three different approaches to the problem.

1) The most simple way is to extract from the machine the low

energy mesons produced in an internal target in the synchro-cyclotron. At Rochester a beam of positive and negative pions of 50 ± 1 MeV is obtained extracting the mesons produced at 160° by the 240 MeV protons which bombard an Al target. The beam is vertically focalized by a magnet.(see Barnes et al.(44) After the mesons are slowed down in the telescope counters and the hydrogeneous target, the final energy is 37 ± 4 MeV. No information is given about intensity etc. For lower energy (see ref. 5 page 29) the beam was moderated by absorbers with a spread of ± 2 MeV.

At Chicago the lowest energy at which the pions are still able to escape the synchro-cyclotron field, is 29 MeV, but the closest channel in the 12 ft iron shield allows only for a 46 MeV pion beam, according to an absorption curve. The beam of negative pions obtained from a Be target has a pion content of 81 ± 3 %, the protons having been filtered out. (See Orear et al. (45) The energy measured on 15 events of scattering found in the plates was 46 ± 3 MeV.

2) A higher energy meson beam, > 40 MeV, is produced internally in the synchro-cyclotron. The mesons are slowed down outside and magnetically analyzed before entering the hydrogen target.

At Chicago (33) attempts were done with the 45 and 90 MeV beam the 90 MeV beam giving much better results. The CH_2 absorber and the nuclear emulsions (target plus detector) were placed at the conjugati foci of a 45° magnetic wedge, which focusing properties improved somewhat the intensity and energy resolution. With this geometry the intensity was 1/80 the intensity without absorber. The negative pion content was 65 ± 4 %. The energy, measured on 5 events was 26 ± 2. A positive pion beam was obtained in the same way (35).

At Nevis the 60 MeV negative pion beam is slowed down in a copper absorber to a mean energy of 15 MeV, with a large spread. The 60 MeV positive pion beam is slowed down in a LiH absorber to an energy of 38 ± 3 MeV (38).

3) A pion beam is produced with the external proton beam, out of the synchro-cyclotron. This has been done only at Berkley (31)(36). Advantage has been taken there of the reaction $p+p \rightarrow \pi^{+}+D$. The external proton beam of 340 MeV strikes a $(CH_2)_x$ target. The produced mesons are monoenergetic in the center of mass system. In the Lab.sys. the energy of the mesons is 70 MeV at 0°, with a maximum spread of $\pm$ 4 MeV. The thickness of the target where the mesons are produced, was chosen to give pions of the desidered energy. It happens that in spite of the finite thickness of the target, the pions at 0° are still nearly monochromatic because of compensation effect between the energy lost by primary protons and the energy lost by the mesons in CH_2. An analysing magnet is used to deflect the pion beam so produced, away from the higher momentum protons.

At Berkley the principle of the spiral orbit spectrometer was also used to focus pions of specified energy emitted at 90° to the incoming external proton beam (46). The authors have claimed an increase in the intensity by a factor 10^3, with an energy spread, for 33 MeV positive pions, of $\pm$ 3 MeV.

In our case the production of pions by the external proton beam was discarded because of the very large background of neutrons and scattered protons.

The slowing down of the pions internally produced, with an absorber in front of the meson deflecting magnet, was also discarded for intensity reasons due to the unreliability of the pulser which controlled the radiofrequency oscillation of the synchro-cyclotron.

It was decided to slow down the 90 MeV positive pion beam in front of the chamber and to analyse the resulting pion spectrum with the $\pi - \mu$ decay method. (See section 7).

* * *

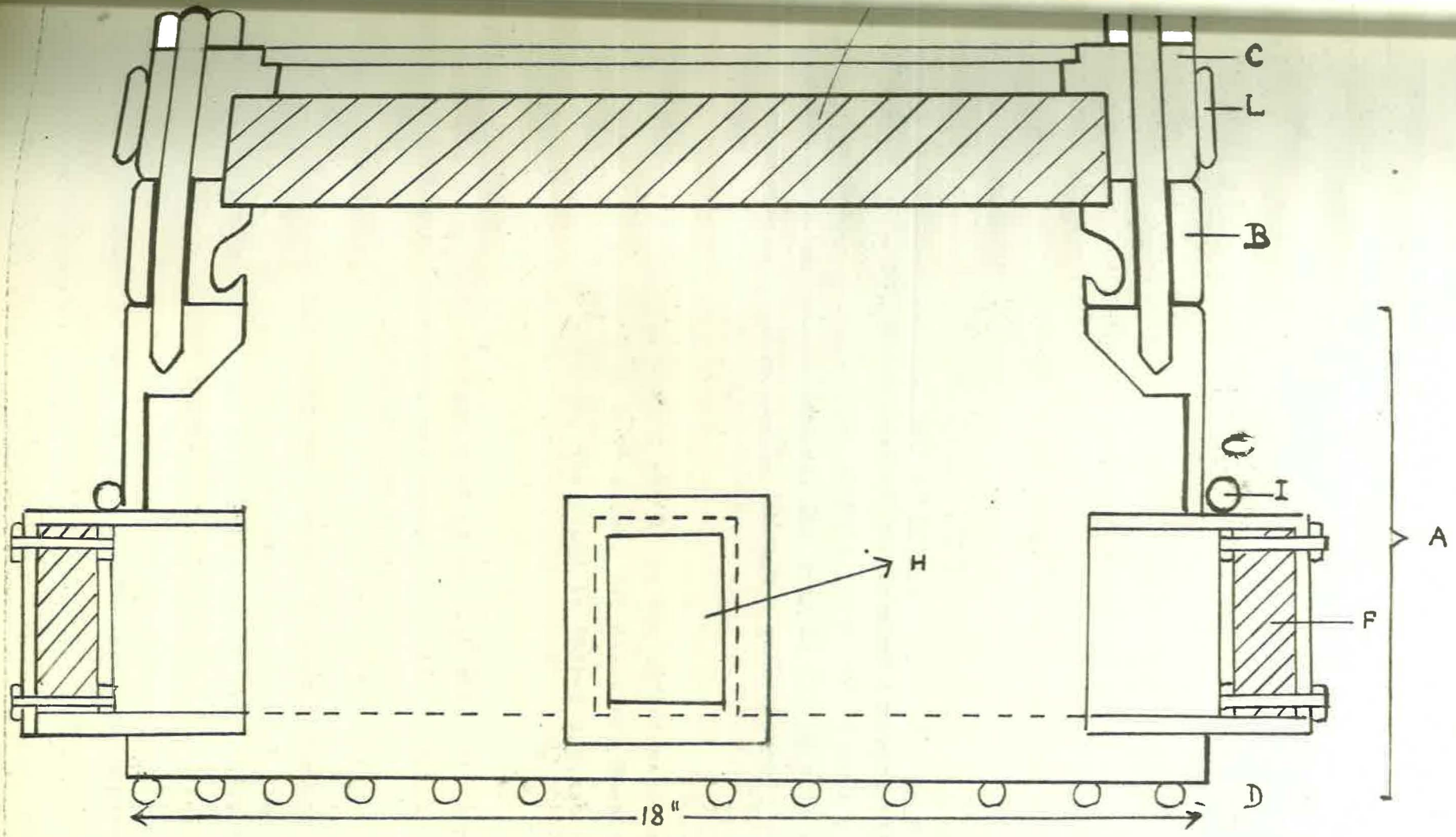

FIG. 3

From M.H. Alston Ph.D. Thesis

5. The Liverpool diffusion cloud chamber

The chamber is made of stainless steel, which is a non-magnetic material, because : a) the low conductivity of this material makes it easier to keep the base cool. b) the chamber can whitstand a high pressure having at the same time thin walls.

The chamber consists of three main parts : A - B - C (fig.3). The bottom part A has a total height of 8". It consists of a base 1" thick and 18" diameter, welded to a cylinder obtained by rolling a 5/16" sheet, which has a 1.5" × 2" ring welded on the top. D is a spiral of 24 ft copper pipe, 0.5" internal diameter, soft soldered to the base, which is needed to cool the bottom of the chamber.

B is the alcohol tray made in cast phosphor bronze, electrically insulated from the rest of the chamber (to apply the clearing field) by two rubber gaskets above and below it, and from the bolts by ebonite bushes. The tray is filled with about 200 cc of alcohol, blown inside through a pipe by means of compressed gas.

Above the tray, between C and B, is the 16" diameter armour plate glass window E, 1.5" thick, 14" diameter. When there is pressure in the chamber, the glass is pushed against the top ring C.

The two 1" thick perspex windows through which the sensitive region is illuminated, are clamped from inside to the ends of two rectangular ports -F- 10" × 4".

The particles can enter the chamber through a rectangular beam entry port, H, 1.5" above the base. The internal size of the port is 2" × 3". In the actual experiment the window is of phosphor bronze, 0.018" thick.

Methil alcohol is used as a vapor. The maximum temperature in-

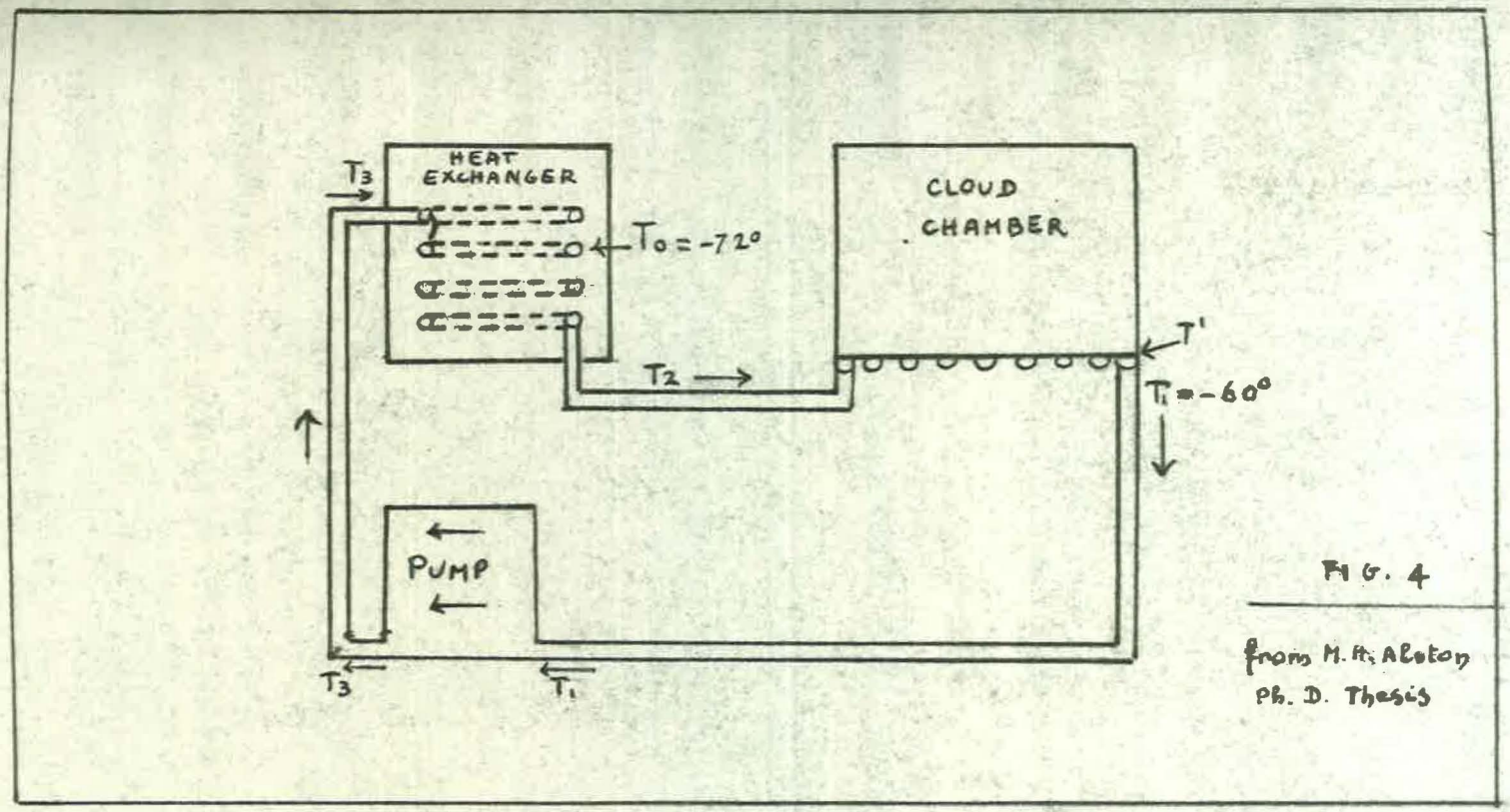

FIG. 4

from M. H. Alston Ph. D. Thesis

OPERATIONAL TEMPERATURE DISTRIBUTIONS

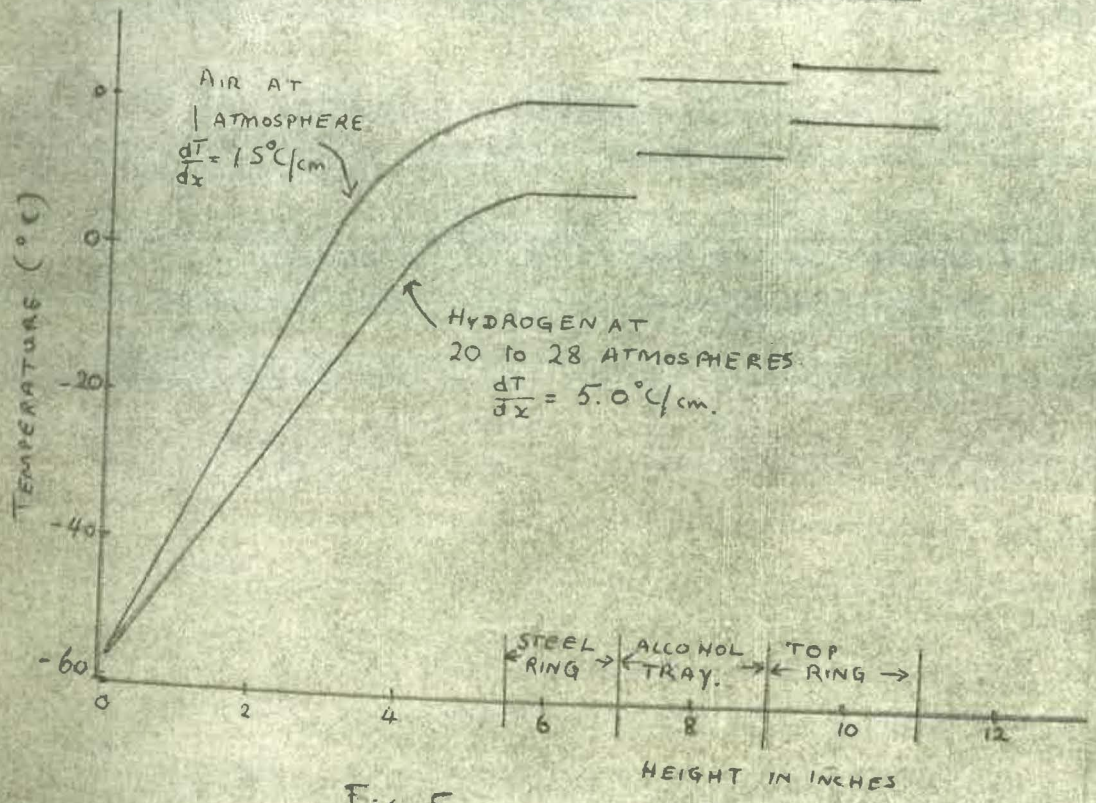

FIG. 5 from M.H. Alston Ph.D. thesis

side the chamber was chosen 25° C, not too close to the boiling point of the alcohol to avoid condensation on neutral centers. The temperature of the top glass is kept uniform to prevent any disturbance in the chamber. The minimum temperature was chosen -60°, in order to maintain a temperature gradient of 5° C / cm, found experimentally as the best one for a 25 atm. hydrogen filled chamber. This gradient gives a sensitive depth of 2.5" - 3", with the normal cosmic ray background. In these conditions there is a heat flow of 50 cal./sec. downwards through the walls, to be taken away. A schematic diagram of the cooling system is shown in fig. 4. The circulating liquid is acetone because of its low viscosity at dry ice temperature. The heat exchanger contains dry ice which evaporates at a rate of about 1 liter of gas per second.

To maintain a uniform temperature gradient there are two electric heaters round the chamber, I and L. The chamber is thermally insulated from the surrounding air by a jacket filled with glass wool 1" thick, and a stream of warm air is directed to the top of the glass, from the top of the cylinder in which the camera is mounted.

The temperature distribution on the walls of the chamber (see fig. 5) is measured by means of thermocouples soft soldered outside the walls at 1" intervals. The current through the heaters is adjusted to the right values. We shall assume that the temperature of the walls is equal to the temperature of the gas on the same horizontal plane. The check of this assumption is obviously quite difficult, because any external body in the chamber will upset the working conditions. Some measurements were done and it seems that the differences in temperature between the walls and the middle cannot be much more than 3° C, and we shall neglect them. Around the walls there is a ring shaped insensitive region 1" - 0.5" large.

The magnetic field for the experiment was 2.3 K gauss. It is produced by passing a current of 900 A through a pair of water cooled Helmotz coils, to give a uniform vertical field in the sensitive region of the chamber. Each coil has a total of 1344 turns. The current generator is designated to give an average rate of

60 Kw. The coil constant was determined, by magnetic measurements, to be 2.55± 0.5 % gauss / ampère, so that the value of the field can be checked at any time by measuring the current in the coils. The current is measured with an accuracy of 1.5 % from the voltage drop across a known resistance, in which a fraction of the main current is derived. The magnetic field in the useful region of the chamber is constant within 3 %.

An intense beam of light is produced by discharging a bank of 400 μ F condensers at 2000 volts, through two Mullard LSD17 flash tubes. These tubes placed near the side windows of the chamber are made of quartz 12" long and 3/8" diameter. The optical system of each tube consists of a cylindrical mirror and a cylindrical convex lens, which make a parallel beam of light to illuminate only the lowest 3" or 4" of the chamber.

The time of growth of the drops is relativelly long because of the low supersaturation, and the tracks become visible about 100 msec after the charged particle has passed through the chamber. To obtain good clear thracks of minimum ionizing particle a longer delay of 300 msec is used. There is very little distor - sion of the tracks, because of the negligible turbulence in the chamber.

A stereoscopic pair of photographs of the events which take place in the chamber is taken through the top window. The camera takes rolls of 70 mm film 100 ft long. The two lenses are of 75 mm focal length and maximum aperture f / 4.5 and are inclined of 13° to each other. The aperture used in the present experiment is f / 16 which gives adequate illumination and good focus over a depth of 3". The field of view of the camera is 16" diameter. The film planes are tilted in respect to the lense planes, and the angle between the film axis is 14°.

5G91 Illford film was used, a high speed panchromatic film. Maximum contrast is required to obtain the tracks to stand out a - gainst the background. Kodak D19B was used as developer, the developing time being ~15 min. The fixing time was about 20 min.

During the operation a negative voltage of 1500 V is normally applied to the alcohol tray, the rest of the chamber being earthed. If we consider pairs of ions formed above the sensitive region, we see that in these conditions the negative ions, which have a higher mobility, are pulled down and so diffuse through the sensitive region in a shorter time than if were the slow positive ions to diffuse downwards.

The timing sequency of the chamber in the actual experiment was :

1) About 5 sec. before the pulsed beam enters the chamber, the alcohol tray is shorted to earth, to take away the clearing field.
2) A signal is sent to the synchro-cyclotron to indicate that a pulse of particles is required. The particles will then start arriving in the chamber within 10 msec, and the required number of synchro-cyclotron pulses can be selected. This number was varied between 4 and 8, according to the reliability of the pulser and of the operating conditions of the synchro-cyclotron.
3) 300-360 msec after the first bunch of particles enters the chamber, the flashes are fired.
4) The voltage which generates the clearing field is switched back on to the alcohol tray.
5) The film is wound on, to prepare the camera for the next exposure.

The recovery time of the chamber after a $\sim$ 20 particles pulse is about 15 sec.; after a pulse of 2 10^4 particles is about 2 min. The recycling time during the present experiment was 10 or 20 or 30 sec., depending on the chamber conditions.

* * *

6. The reprojection set up

The reprojection set up makes use as a projector of the same camera which is used to take the pictures of the events in the diffusion chamber. Both the stereoscopic pictures can be pro-

jected at the same time into a screen which can be rotated and moved up and down, for a threedimensional reconstruction of tracks, and also to find the plane in which a scattering or a $\pi - \mu$ decay occured. For an accurate reconstruction of the events, a glass 1.5" thick is inserted between the screen and the projector to simulate the glass window of the diffusion chamber through which the pictures are taken.

Moreover, as the optical axis of each lens is inclined in respect to the vertical, a better focusing is obtained rotating the film in respect to the plane of the lens, by a small angle, as it is shown in fig. 6. The proof is immediate. This argument holds, of course, both to take the pictures and to reproject the events.

* * *

7. Analysis of the photographs. The pion spectrum.

We had three runs with the synchro-cyclotron for a total time of about 100 hours.

In the first run we used as a moderator 1.532" of copper, and in the last two runs 9.75" of CH_2. The copper moderator because of the higher Z, should give a larger radial displacement of the pions entering the chamber, which would make the scanning easier. On the other hand, the energy spread is increased, because the path lengths of the pions through the moderator have a larger spread(*).

(*) The energy loss is proportional to NZx and the mean square angle (θ^2) to NZ^2x, where N = number of atoms/cm^3, Z = atomic number and x = thickness in cm. (Ref. 42, vol.1, page 242). For the same loss of energy (θ^2) becomes larger, if Z increases.

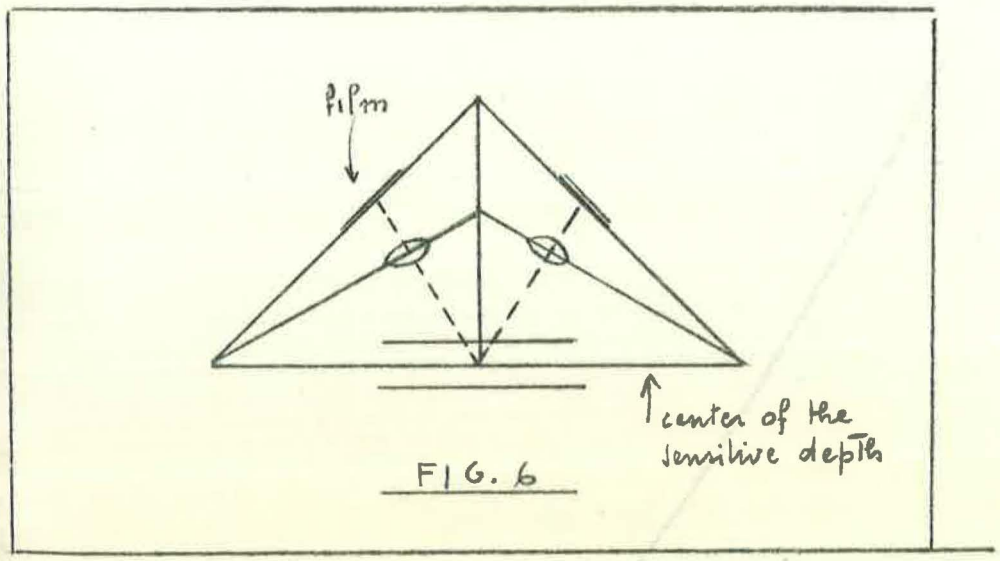

FIG. 6

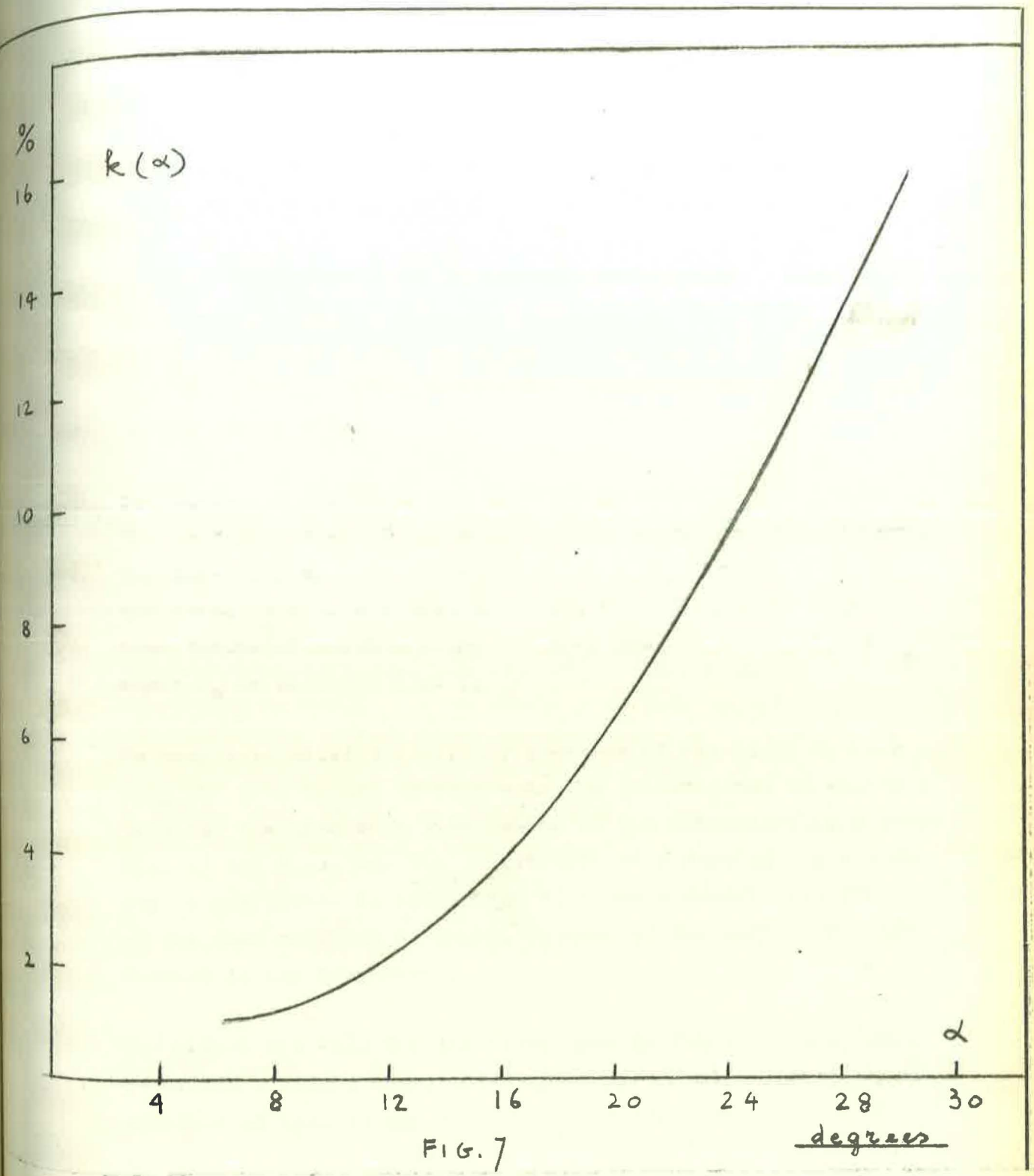

FIG. 7

During the runs, the pressure and the temperature of the chamber were carefully checked. The operating conditions were :

run	pressure	mean temperature in the sensitive region	mean gas density
1	24.8 atm.	- 35° C	2.54 mg cm^{-3}
2	26.7 "	- 35° C	2.74 " "
3	25.8 "	- 35° C	2.64 " "

We have taken 5400 pairs of stereoscopic pictures. First both pictures of a pair were scanned in a horizontal plane, searching at the same time for $\pi \rightarrow \mu$ decays and $\pi \rightarrow p$ scattering events. Later all the pictures were rescanned for π - p scattering events only.

The radius of curvature was measured by means of a template. The precision was 2 % for pions in the energy range 5- 40 MeV. The dip angle α, i.e. the angle which a track makes with the horizontal plane, was also measured. The relation between the true radius of curvature and the measured one is $r_t = r_m (1-k_\alpha)$, where k_α is given in fig. 7.

We have determined the primary spectrum of the pions by counting the pion decays in each momentum interval and by correcting for the pion mean life, which in the laboratory is a function of the momentum. The probability of observing a μ - e decay is negligible in comparison to observe decays from pions of the same momentum as muons, because of the very large difference in the mean lives.

The method was used for the first time by Fowler et al. (48). It avoids a direct measurement of the muon and electron contamination as well as any calibration of the beam entering the chamber. It is not possible to distinguish between pions and muons on the base of ionization and radius of curvature as the tracks in a diffusion chamber are practically continuous, due to the high value of the ionization and it is not possible to do ionization measurements. Obviously it is not possible to recognize pions and muons only by means of the curvature.

The method has the further advantage that, if we suppose that the probability of seeing a pion decay is the same as the probability of seeing a scattering event (*), it corrects automatically for non uniformities in the efficiency through the chamber. If we had to monitor the beam at the entrance of the chamber it would have been necessary to introduce a cor - rection for the geometry of the chamber, the illumination and so on.

Let us look at the method in more detail, Let us put :

N = number of meson which enters the chamber,

K = probability that they can be observed looking at the screen.

This probability is smaller than one because of the above mentioned reasons.

The probability for observing a meson is the same whatever its fate in the chamber. Thus the apparent number of pions which enter the chamber is KN.

The possible processes for low energy positive pions are :

a) decay into a muon.

b) scattering by a hydrogen nucleus caused either by nuclear or Coulomb forces.

c) interaction with complex nuclei because of the presence of alcohol in the chamber.

Production of mesons is excluded for energy reasons. a) is quite well known. b) is the process we are looking for, and we know the order of magnitude of the cross section. In the range of energy, we consider, the probability for process. b) is much smaller than the probability of process. a) by at least a factor 100. c) is not important because the number

---

(*) This is not really true because of the very heavily ionizing prong in a scattering event and of the quite different angular distribution of the scattered pions and the decay muons.

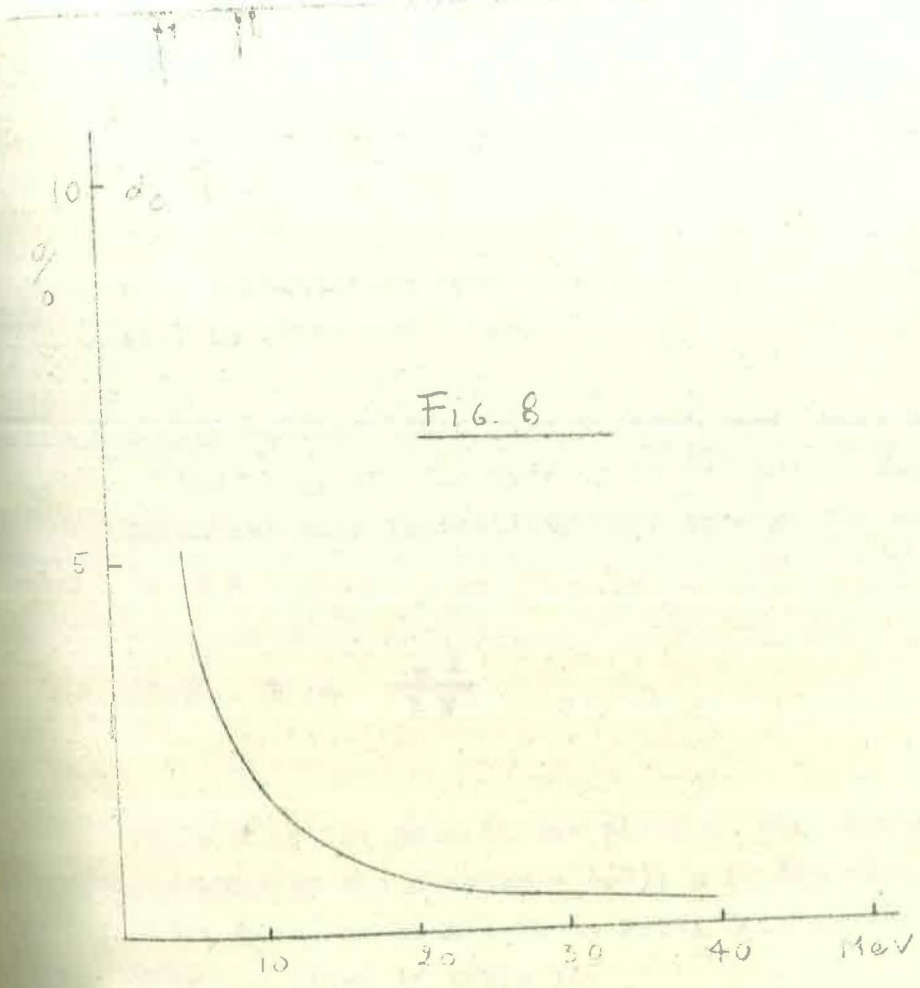

FIG. 8

of complex nuclei present in the chamber is very small and in any case the interactions with complex nuclei are easily recognized.

It is possible to calculate the probability P for process a) in any energy interval ΔE. ΔE can be as small as we like, the only restriction coming from the available statistics. The apparent pion spectrum will be :

$$k \frac{\Delta N}{\Delta E} = \frac{\text{number of observed decays in } \Delta E}{\text{decay probability in } \Delta E} \cdot \frac{1}{\Delta E} .$$

This is the spectrum which has to be used for the derivation of the scattering cross section, a part from correction which will be discussed later.

The probability of a pion decay depends only on the momentum of the pion, and the density of the gas in the chamber can influence this probability only through the momentum p. It is :

$$(39) \qquad P = \frac{\mu \ell}{p \tau}$$

where ℓ is the path of the pions in the chamber ($\sim$ usefull diameter of the chamber = 16"); μ is the rest mass of the pion; τ is the mean life at rest. Some numerical values for $\mu/p\tau$ are given in table II.

The formula (39) has been obtained with the assumption that the variation in momentum of the pion going through the gas of the chamber is small. This is certainly correct for pions of energy greater than 10 MeV.

The total track length in a specified momentum interval Δp is :

(40) $$L = \frac{\text{number of observed decays in } \Delta p}{\mu / pr}$$

which is easily related to the track length in a specified energy interval ΔE.

The pion spectrum so determined has to be corrected for : a) Coulomb scatterings which look like pion decays b) scanning inefficiency. The correction a) has been claculated in Appendix B and the results are condensed in the graph (fig.8).

The scanning inefficiency consists of :
1) true inefficiency : the observer just misses a decay
2) intrinsic inefficiency of the method. We assumed that pion decays with a projected angle in the horizontal plane less than 5° in both the two stereoscopic pictures, were missed by the observer.

1) was determined experimentally, repeating the scanning by two independent observers. 1000 pairs of pictures were rescanned for pion decays. Combining the pion decays obtained in the two scans, after a comparison, we assumed a 100 % efficiency for all the decays with projected angle larger than 5°. We estimated scanning efficiencies of 82 % and 94 % in the first and second scan respectively. We did not find any evidence for a variation of the efficiency in the energy spectrum and found no systematic difference between the 1st run and the 2nd and 3rd.

2) is evaluated in Appendix A, and the results are summarized in the diagram (fig. 9).

The results are given in table III. The corrected pion spectrum is shown in fig. 10.

* * *

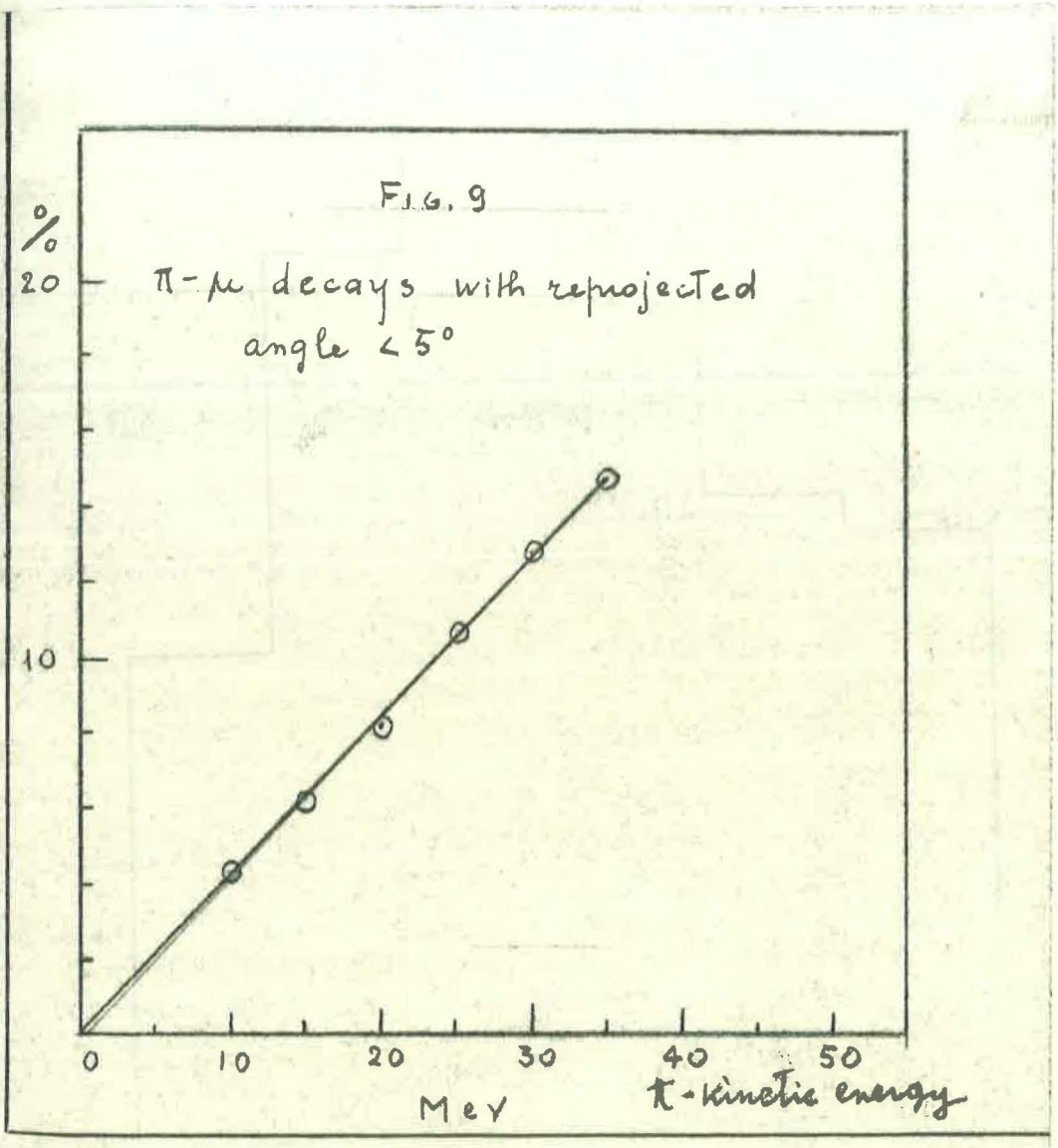
%
20
10
π-μ decays with reprojected angle < 5°
0
10
20
30
40
50
MeV
π-kinetic energy

FIG. 9

FIG. 10

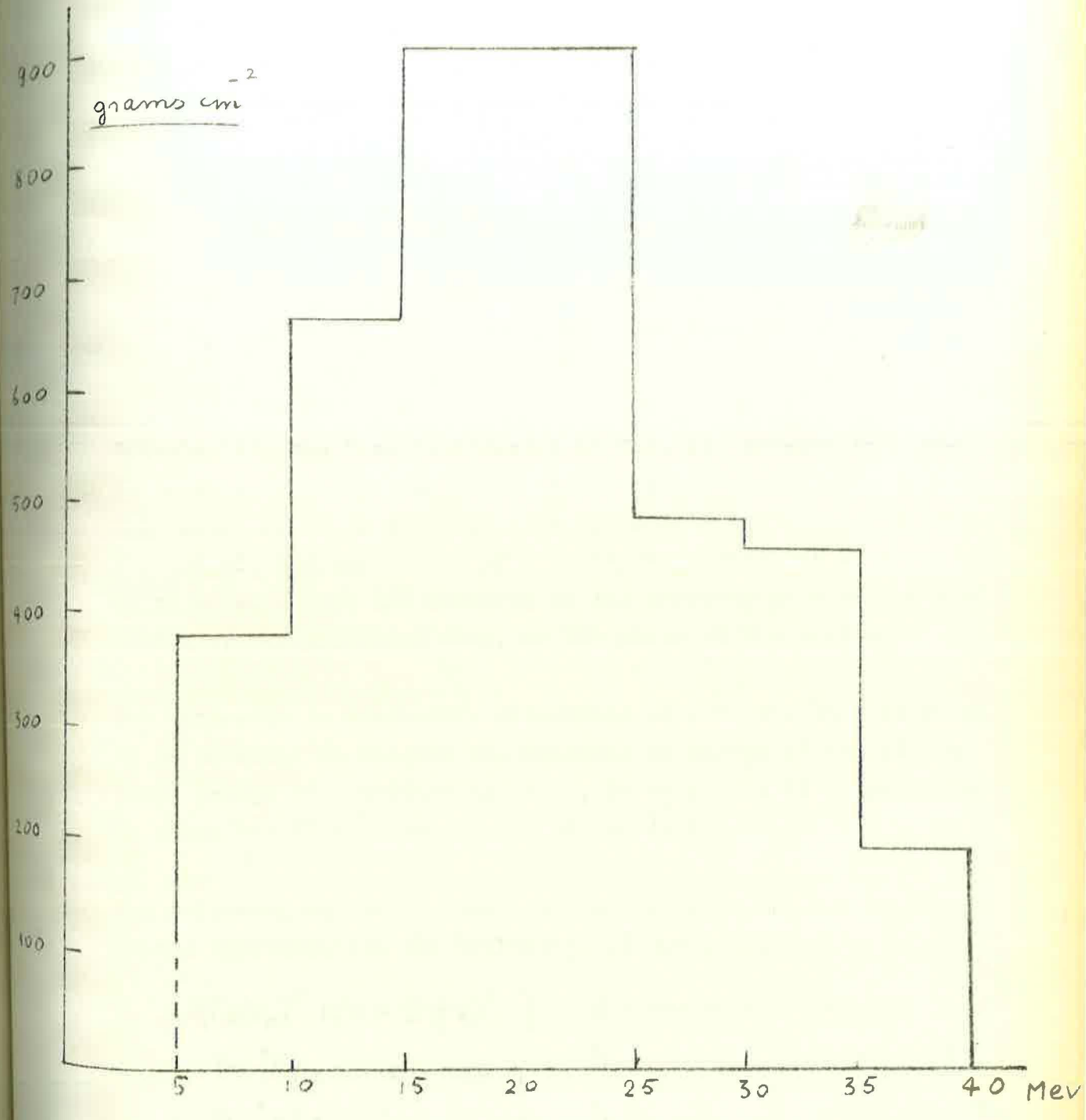
900
grams cm⁻²
800
700
600
500
400
300
200
100
5
10
15
20
25
30
35
40 Mev

8. Analysis of the scattering events

Any event looking like π - p scattering was accurately studied to see if the kinematic was correct. The three prongs have to be coplanar. Moreover the scattering angle and the recoil an - gle have to satisfy a relationship, which in the non-relativis- tic aproximation, is independent of the energy and is establi- shed once the mass of both particles are known.

$$(41)\quad \sin^2\theta_\pi = M/\mu \frac{1-\cos^2\theta_p}{\cos^2\theta_p/a+1} \cos^2\theta_p/a \quad \text{where } a = (\mu+M)^2/4\mu M$$

μ = mass of the pion M = mass of the proton

θ_π = scattering angle θ_p = recoil angle

Formula (41) has been represented in fig. 11. Because this re- lationship is independent from the energy, the kinematic is not determined if it is possible to measure only two angles. To de- termine all the parameters of a scattering event, it is necessa- ry to measure also the momentum of the incoming pion or the mo- mentum of the scattered pion, or the range of the proton.

The kinematic is completely determined also in the case in which it is possible to measure the momentum or energy of two of the three prongs of a scattering event. In this case it is possible to check the direct measurement of the angles.

The following equations summarize entirely, in the non relati- vistic approximation the kinematics of π - p scattering :

$$\left.\begin{aligned} &1+(\rho_p/P_\pi)^2\ \mu/M = (P/\rho_\pi)^2 \\ &\cos\theta_\pi + \rho_p/\rho_\pi \cos\theta_p = P/\rho_\pi \\ &\sin\theta_\pi + \rho_p/\rho_\pi \sin\theta_p = 0 \end{aligned}\right\}$$

P = momentum of incoming π

ρ_π = " " scattered π

ρ_p = " " recoil proton

Fig. 11, together with fig. 12 and fig. 13 give a complete gra - phical representation of the above system of equations.

* * *

FIG. 11

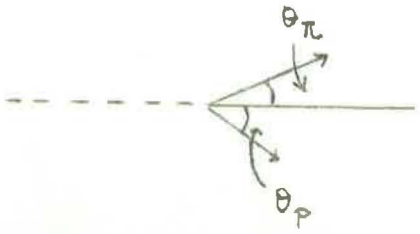
θ_π
θ_p

180
170
160
150
140
130
120
110
100
90
80
70
60
50
40
30
20
10
10
20
30
40
50
60
70
80
θ_p degrees
100
110
120

FIG. 12

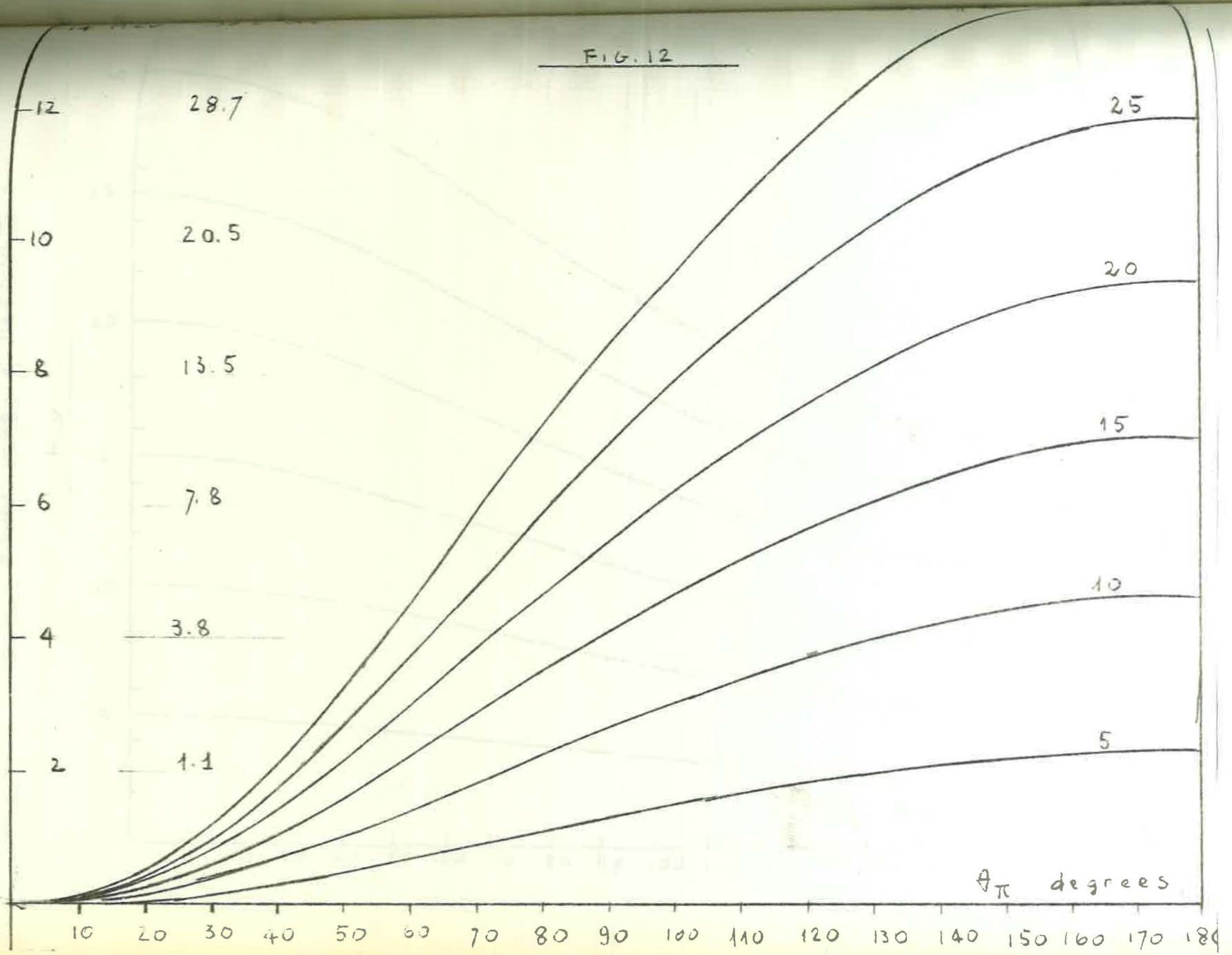
12
10
8
6
4
2
28.7
20.5
13.5
7.8
3.8
1.1
25
20
15
10
5
θ_π degrees
10 20 30 40 50 60 70 80 90 100 110 120 130 140 150 160 170 180

FIG. 13

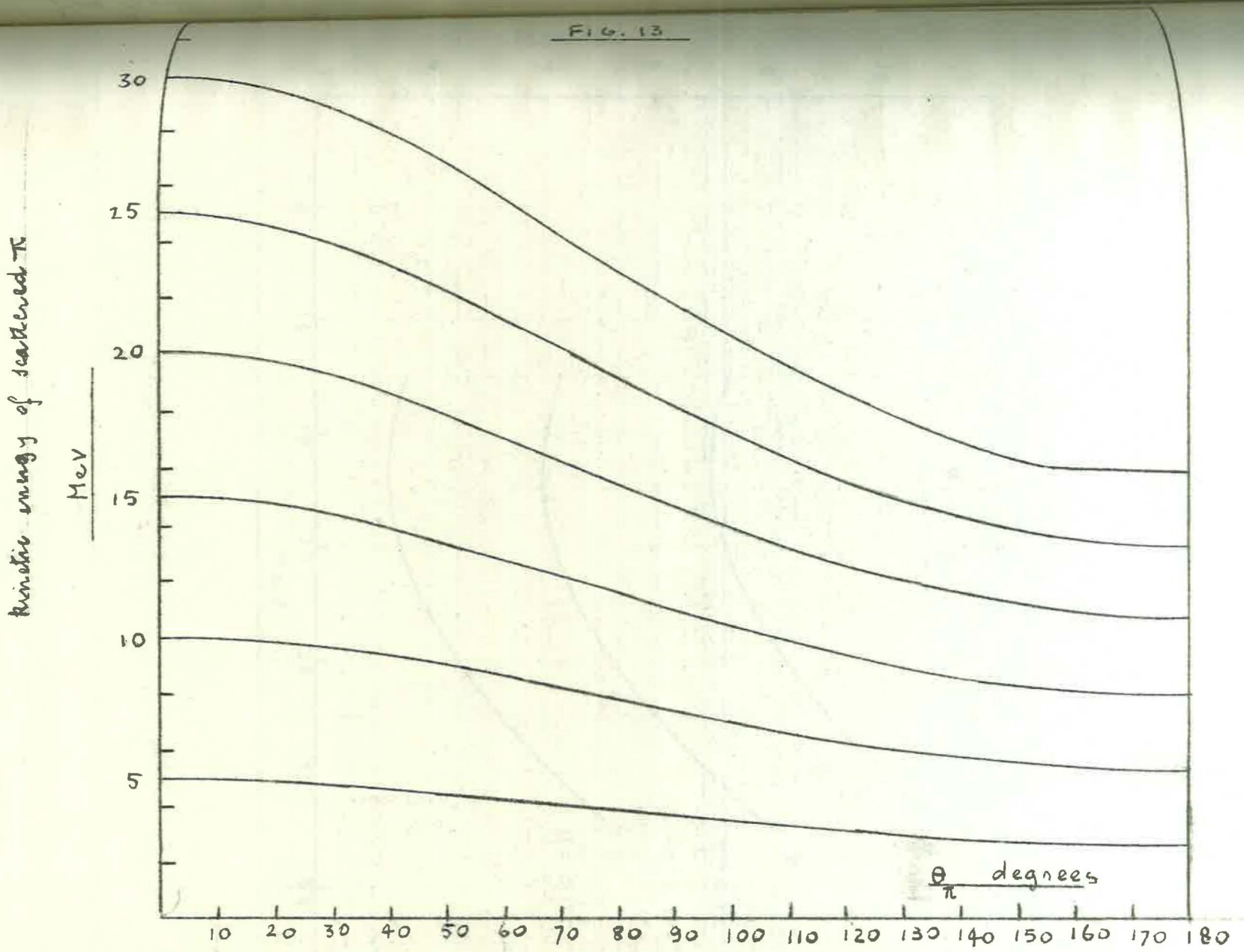
Kinetic energy of scattered π
MeV
30
25
20
15
10
5
θ/π degrees
10 20 30 40 50 60 70 80 90 100 110 120 130 140 150 160 170 180

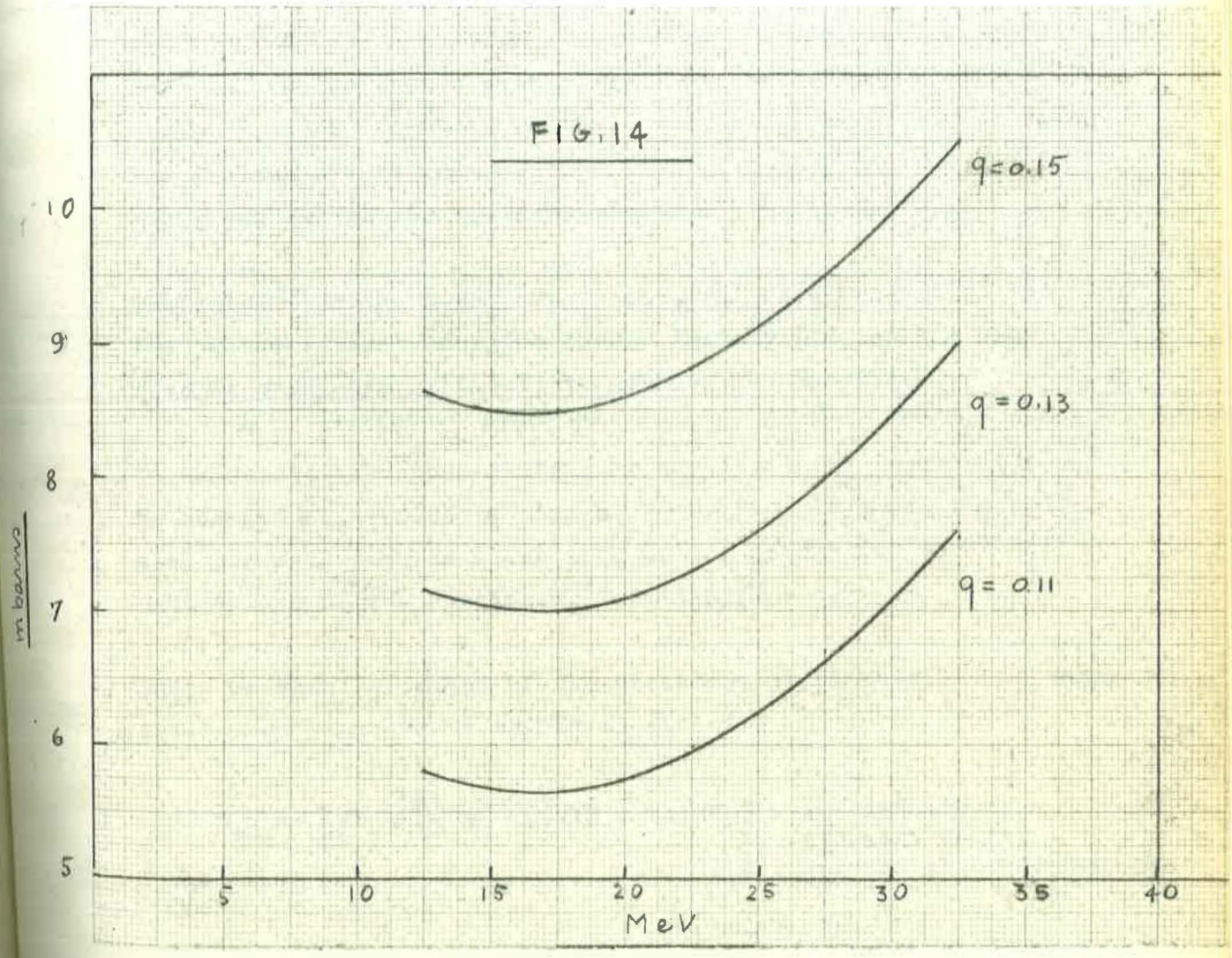
FIG. 14
q=0.15
q=0.13
q=0.11
10
9
8
7
6
5
millibarns
5
10
15
20
25
30
35
40
MeV

9. Results

We have found 15 π^+-p scattering events with incident energy in the range 10 - 35 MeV, and with scattering angle > 60° in the c.m.s. (*) (See table IV) Fig.20 shows a photograph of an event.

The lower energy cut-off was introduced in order to consider only scattering events with clearly visible tracks (longer than 0.5 cm) for protons recoils, and at the same time to reduce the Coulomb effect (See section 1 of part II). The cut-off in angle was chosen for the same reasons.

The cut-off on the high energy side, was used because of the few pion decays at energies larger than 35 MeV. At the same time it gets more difficult to measure the moments.

To calculate the cross-section we have used the formula (38). We assumed $\alpha_{33} = 0.235\,\eta^3$ and $\alpha_{31} = 0$. Fig. 14 shows the integral cross-section as a function of the energy for three different values of the scattering length $\alpha 3/\eta = q$.

Since we know the shape of the spectrum, it is possible to calculate how many events we had to expect.

$$n_{exp} = \sum_E \rho N \cdot \frac{\Delta L}{\Delta E}\, \sigma_q(E)\, \Delta E$$

where ρ = gas density
N = avogadro number
$\sigma(E)$ = calculated cross-section

Using this formula the expected number of events in the three cases is :

q	expected number of events
0.11	12.75
0.13	15.35
0.15	18.40

(*) At our energies this angle corresponds, with a very good approximation, to 52° in Lab-system.

FIG. 15

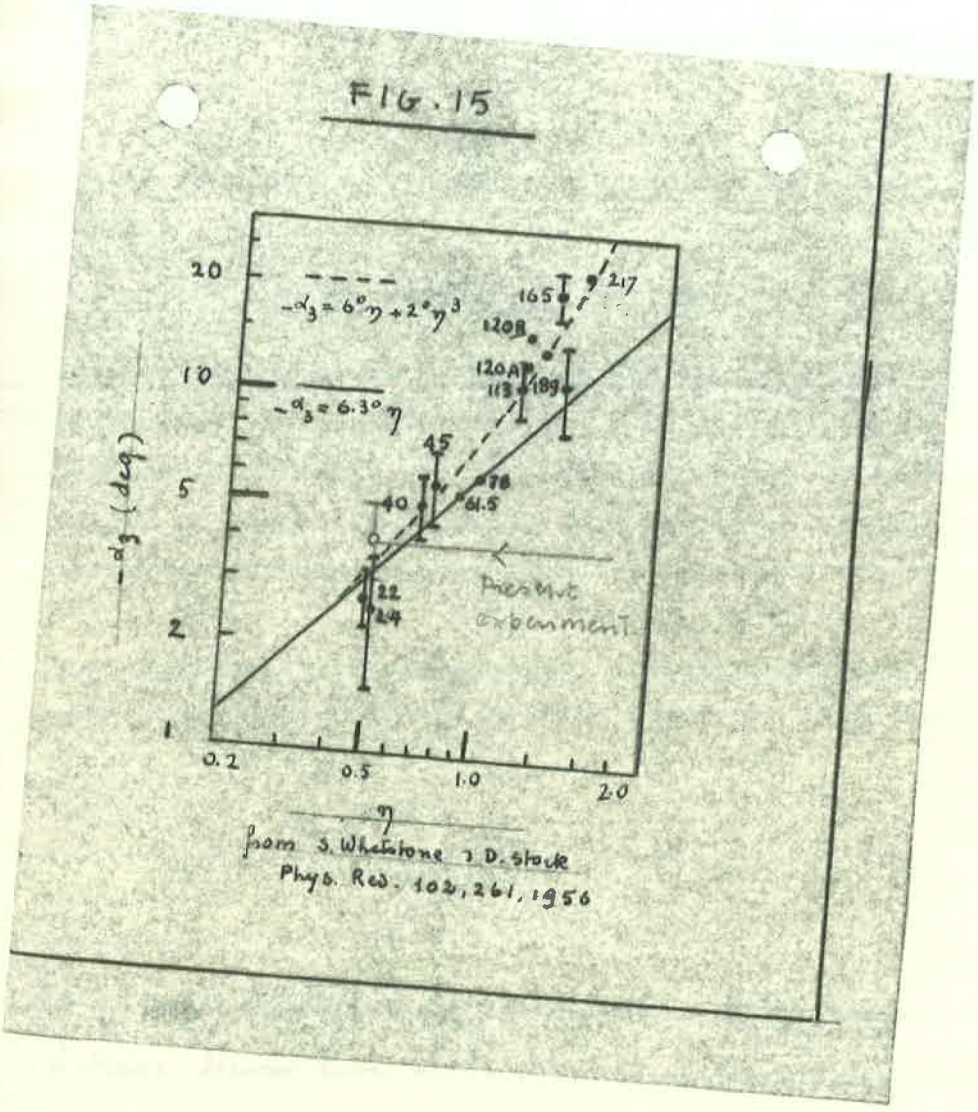

from S. Whetstone & D. Stork
Phys. Rev. 102, 261, 1956

By comparisons of these values with our experimental result we find $q = 0.13 \pm 0.030$, where the error is only the statistical one. We have estimated that it is necessary to add to the statistical error a systematic experimental error of the order 5%. This systematic error includes contributions from inaccurate knowledge of gas density, scanning efficiency and spectrum corrections.

We have also estimated that by assuming $\alpha_{31} = 0$, we introduce a negligible error, less than 1 % if we admit that α_{31} which is known to be rather small, were as large as 1°.

Taking into account these considerations we get for the final value :

$$-\alpha_3 = (0.13 \pm 0.035)\,\eta$$

in good agreement with the analysis by Orear ($\alpha_3 = -0.11\eta$) and by Whetstone and Stork ($-\alpha_3 = 0.105\eta + 0.035\,\eta^3$) (See fig. 15). In this figure, we have reported also our experimental point, at an energy equal to 24.4 MeV ($\eta = 0.526$) which is the average energy calculated from the 15 scattering events.

The experimental cross-section, directly computed from the 15 events we observed and the pion spectrum, is 7.4 mbarns.

* *

*

In a paper published at completion of the present work (J. Orear, Nuovo Cim. 4.856.1956) Orear has analyzed with a least squares method, the experimental data on π-p scattering in the range 0-58 Mev, available up to the summer 1956

He finds $\alpha_1 = (0.167 \pm 0.012)\,\eta$ $\alpha_3 = -(0.105 \pm 0.010)\,\eta$

where the results of the present experiment as well the new Panofsky ratio have been taken into account.

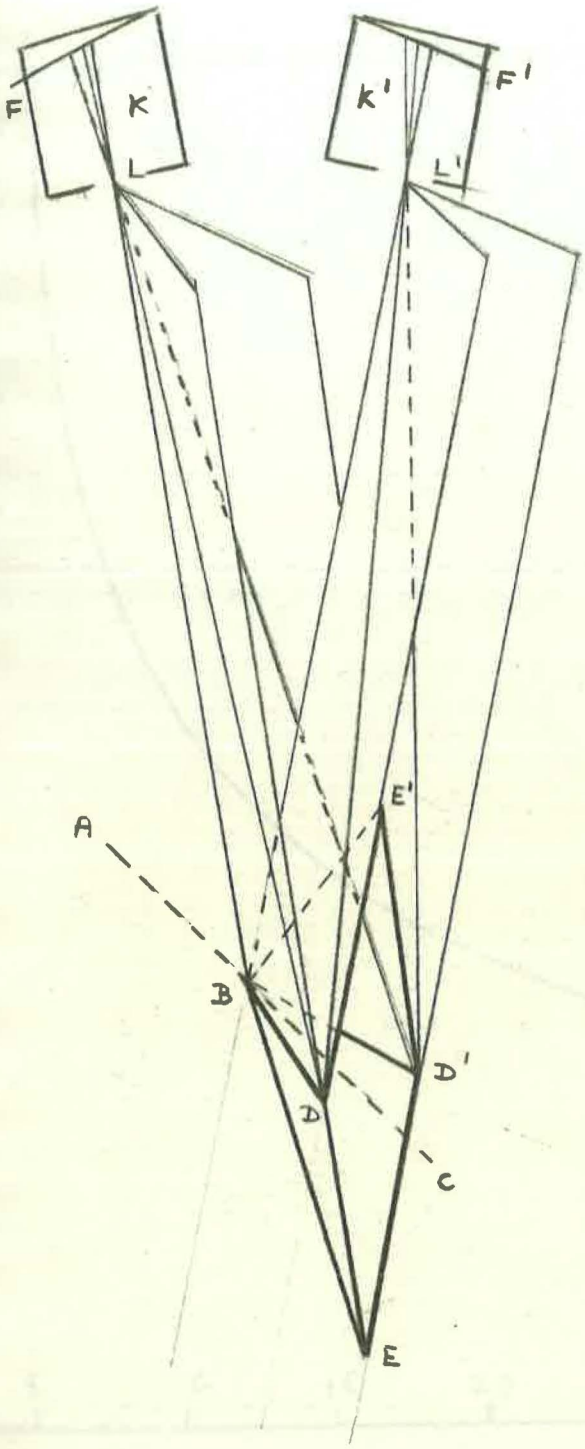

FIG. 16

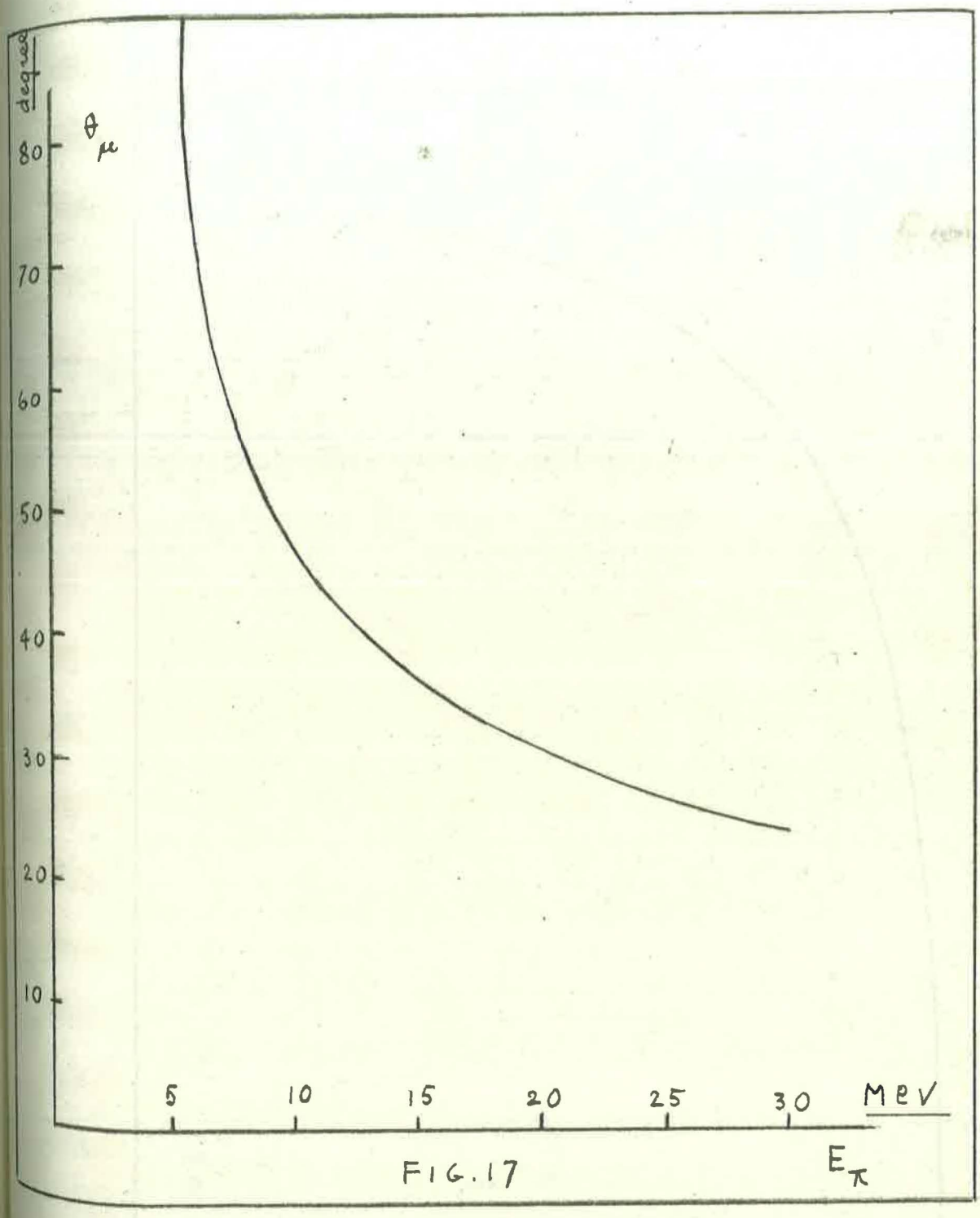

FIG. 17

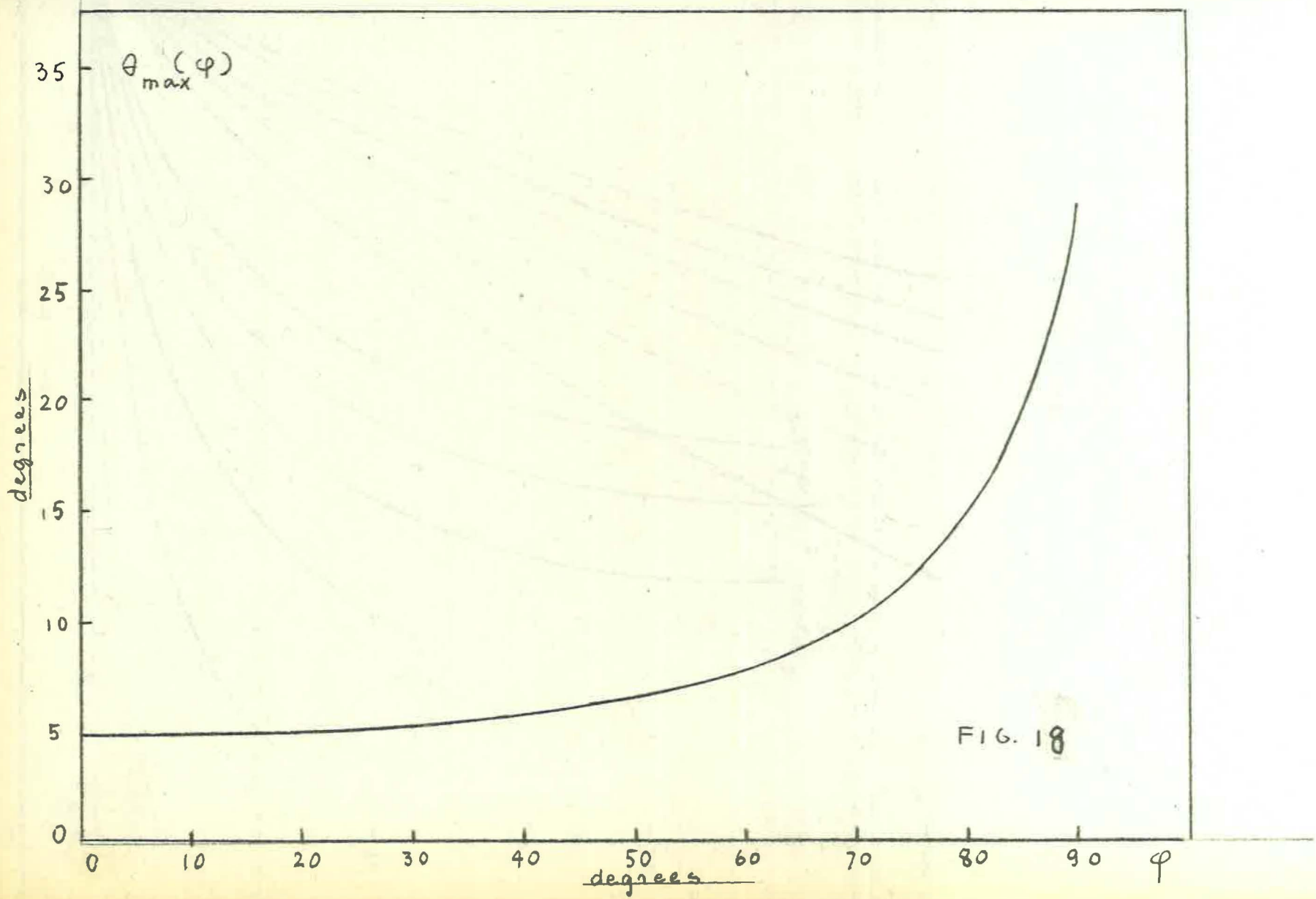
$\theta_{max}(\varphi)$
35
30
25
20
15
10
5
0
degrees
0
10
20
30
40
50
60
70
80
90
φ
degrees

FIG. 18

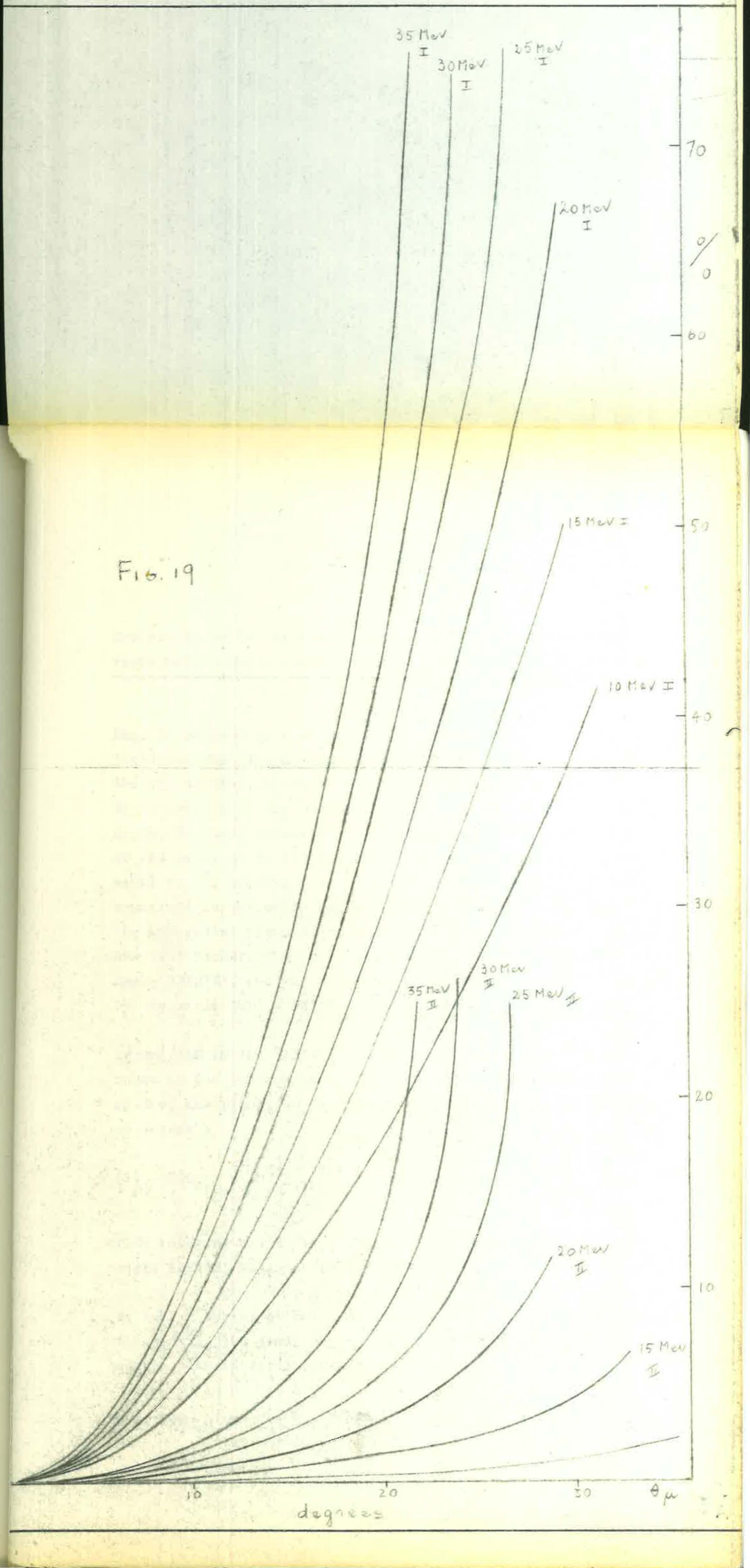
35 MeV I
30 MeV I
25 MeV I
20 MeV I
15 MeV I
10 MeV I
35 MeV II
30 MeV II
25 MeV II
20 MeV II
15 MeV II
70
60
50
40
30
20
10
%
0
10
20
30
θμ
degrees

Fig. 19

APPENDIX A

Correction to the spectrum assuming that $\pi - \mu$ decays with a reprojection angle smaller than 5° are missed during the scanning.

Fig. 16 represents a geometrical reconstruction of the optical trajectories when $\pi - \mu$ decays are being photographed. K and K' are the two cameras, F and F' the planes of the film, L and L' the optical centers of the lenses, C is the center of the sensitive depth. We shall assume that all the pions travel in the direction AC and decay at B. $\hat{DBC}$ and $\hat{CBD}$ in the horizontal plane are each equal to 5°. Looking from L and L', we suppose that all the muons contained in the solid angle BDED'E' and therefore projected into the horizontal plane at an angle $< 5^\circ$ with the pion direction, are lost because they are missed during the scanning. The solid angle $\hat{BDED'E'}$, and therefore the correction also, is determined by the angle $\hat{DED'} = \hat{DE'D'} = \hat{LCL'}$, which we shall take = 18°.

If $dn / d\Omega$ is the differential angular distribution of decay muons in the laboratory system, which is a function of the energy E of the pions, we have for the pecentage $F(E_\pi)$ of missed pion decays :

$$(1) \qquad F(E_\pi) = \int {}^{dn}/_{d\Omega}\, d\Omega$$

This integral has to be calculated over that part of the solid angle $\hat{BDED'E'}$ which contains decay muons.

We take a system of polar coordinates : BC is the direction of the z-axis, the decay angle is θ, and φ is measured around the z-axis. The integral (1) becomes :

$$(2) \qquad F(E_\pi) = \tfrac{1}{2}\pi \int_0^{2\pi} d\varphi \int_0^{\theta\,\max(\varphi)} {}^{dn}/_{d\Omega}\, \sin\theta\, d\theta$$

$\theta max\ (\varphi)$ is always given by one of the two following determinations :

$$(3) \quad \theta_{max}\ (\varphi) = \text{artg} \left\{ \text{tg } 5^\circ \ \frac{\cos 9^\circ}{\cos(\varphi - 9^\circ)} \right\}$$

$$(4) \quad = \text{artg} \left\{ \frac{\beta^*_\mu / \beta_\pi}{\sqrt{1-(\beta^*_\mu / \beta_\pi)^2}} \cdot (1-\beta_\pi^2)^{\frac{1}{2}} \right\} \ (*)$$

The first one is purely geometrical : here, as φ increases $\theta max\ (\varphi)$ also increases, but cannot be made larger than the value assigned by (4), as this is the maximum decay angle of a muon in the lab. sys. for pions of given energy. Fig.17 shows a graph of (4) as a function of the kinetic energy of the pion E_π. Fig.18 shows a graph of (3) as a function of φ.

If we call $N(\theta)$ the integral angular distribution of the decay muons, i.e. the fraction of muons which decay at an angle $\leq \theta$ (including pions which decay backward and forward in c.m.s.) :

$$(5) \quad N(\theta) = \tfrac{1}{2}\left[1-\cos\theta^*_1\ (\theta)\right] + \left\{1-\tfrac{1}{2}\left[1-\cos\theta^*_2\ (\theta)\right]\right\}$$

Where θ^*_1, and θ^*_2 are the smaller and the larger value, respectively of θ^* which corresponds to the same value ofθ, (**) the integral (2) becomes :

(*) Here, and in the following, all the symbols with * refer to c.m.s.

(**) The relation between θ^* and θ is :

$$\text{tg}\,\theta = \frac{\beta^*_\mu \sin\theta^*}{\beta^*_\mu \cos\theta^* + \beta_\pi} \ (1-\beta_\pi^2)^{\frac{1}{2}}$$

$$(6) \quad F(E_\pi) = \frac{1}{\pi}\int_0^{2\pi} N\left[\theta_{max}(\varphi)\right] d\varphi$$

Fig. 19 shows the integral angular distribution calculated for several energies of the pion. I and II correspond to the two terms of (5).

Let us call φ^o the φ coordinate at which (3) gets equal to (4), we have :

$$(7) \quad F(E_\pi) = 2/\pi\int_0^{\varphi_o} N\left[\theta_{max(\varphi)}\right] d\varphi + (1-2\varphi_o/\pi)$$

where θ_{max} is given by (3).

The integral (7) can be easily calculated numerically. Assuming $D\hat{E}D' = 18^o$, and combining the graphs of fig. 17 and 18, φ_o can be found for any energy E_π.

If E_π is so small that φ does not exist, the correction is obviously given by :

$$(8) \quad F(E_\pi) = 2/\pi\int_0^{\pi/2} N\left[\theta_{max(\varphi)}\right] d\varphi$$

The correction $F(E_\pi)$ is shown in fig. 9.

* * *

APPENDIX B

Single Coulomb scatterings of pions in hydrogen mistaken for pion decays.

The probability for a Coulomb scattering in hydrogen, at an angle θ^* in c.m.s. in the elementary solid angle $d\Omega^*$ is given by :

$$(1) \quad W(\theta^*)\, d\Omega^* = N/4\, r_e^{\,2} \left(\frac{m_e c}{\beta_\pi p_\pi^*}\right)^2 \frac{d\Omega^*}{\sin^4\theta^*/2} \quad (\text{grem}^{-2})^{-1}$$

where N = Avogadro's number.

r_e = Classical radius of the electron.

$m_e c^2$ = Mass of the electron.

Looking at fig. 16, a Coulomb scattering is mistaken for a pion decay, if the pion is scattered outside the solid angle $\hat{B}DED'E'$.

We suppose that fig. 16 refers to the c.m.s. In this case the angle $D\hat{B}C$ will be 6°, which corresponds at low energy to 5° in the lab.sys.

The probability of Coulomb scatterings per (gr cm^{-2}) of hydrogen, mistaken for pion decays is given by :

$$(2) \quad C = N/4\, r_e^{\,2} \left(\frac{m_e c}{\beta_\pi p_\pi^*}\right)^2 \int_0^{2\pi} d\varphi^* \int_{\theta^*(\varphi)}^{\pi} \frac{\sin\theta^* d\theta^*}{\sin^4\theta^*/2} \quad (\text{gr cm}^{-2})^{-1}$$

in analogy with Appendix A, except that here it is :

$$(3) \qquad \theta^*(\varphi) = \text{artg}\left\{\text{tg } 6^\circ \frac{\cos 9^\circ}{\cos(\varphi^* - 9^\circ)}\right\}$$

With good approximation it is :

$$(4) \qquad \int_{\theta^*(\varphi)}^{\pi} \frac{\sin\theta^* d\theta^*}{\sin^4 \theta^*/2} \simeq \frac{2}{\sin^2 \theta^*(\varphi)/2}$$

From (3) we see that the maximum value for $\theta^*(p)$ is $33^\circ 30'$ so that it is still possible, after the integration in respect to θ^*, to approximate $\text{tg}\theta^*(\varphi) \sim \sin\theta^*(\varphi) \sim \theta^*(\varphi)$, with a maximum error of $\simeq 10$ % at $\varphi = 90^\circ$. Therefore we can write :

$$\sin^2\left\{\theta^*(\varphi)/2\right\} = \frac{1}{4}\left\{\frac{\text{tg } 6^\circ \cos 9^\circ}{\cos(\varphi^* - 9^\circ)}\right\}^2$$

Performing the integration in respect of φ we get :

$$\int_0^{2\pi} d\varphi^* \int_{\theta^*(\varphi)}^{\pi} \frac{\sin\theta^* d\theta^*}{\sin^4 \theta^*/2} = 2300$$

Therefore : $C = 2300\ N/4\ r_e^2 \left(\frac{m_e c}{\beta_\pi p_\pi^*}\right)^2 \left\{\text{gr cm}^{-2}\right\}^{-1}$

If the gas density is 2.6 gr cm^{-2}, $C = 1.83\ 10^{-3} / (p^* \beta)^2\ \text{cm}^{-1}$. The diagram of fig. 8 gives the ratio αc of C to the probability of a decay per cm, as a function of the kinetic energy of the pion.

* * *

(*) A Coulomb scattering cannot really be mistaken for a pion decay if the recoil proton is visible. However a fairly large scattering angle corresponds to a recoil proton with a range larger than, say 0.5 cm. Because of the small contribution to (2) from large angles, the integration in respect to θ^* can be performed up π, without appreciable error.

APPENDIX C

Essential datas of the Liverpool synchro-cyclotron

Magnet internal diameter : 156" (*)

Magnetic field : 18275 $\pm$ 25 gauss.

Number of pulses per sec. : 100

Pulse length : 60 μ sec. for protons,
120 μ sec. for pions.

Available beams : 383 MeV protons.

The internal current is 1μA.

The external current of 2 10^{-2} μA, corresponding to 4 10^{10} protons cm^{-2} $sec.^{-1}$, is focused on to an area of 0.5 sq.in., at a distance of 20 ft from the focusing magnet.

Neutrons from 200 to 400 MeV.

95 MeV negative and positive pions. Positive pions are obtained internally with a copper target 4".1.5".0.25". Negative pions are obtained with a beryllium target. The targets were chosen and adjusted empirically : the yield of pions at a certain angle and a certain energy depends on the atomic weight in a complicated way (See H.A. Bethe, F. de Hoffmann, S.S. Schweber, Mesons and Fields, Vol.II, page 343).

*

* *

(*) Actual magnet diameter is 156", but only 138" can be used because of obstruction by the proton extraction assemblees.

TABLE I

Particle	$e^{\pm}$	$\mu^{\pm}$	π^{+}	π^{-}	π^{o}	p	n
Mass g	$9.1085 \pm 0.0006\ 10^{-28}$						
MeV	0.510984 ± 0.00002	105.8 ± 0.2	139.7 ± 0.1	139.2 ± 0.1	134.7 ± 0.3	938.232 ± 0.024	939.526 ± 0.024
m_e	1	206.9 ± 0.2	273.3 ± 0.2	272.8 ± 0.3	263.7 ± 0.7	1836.13 ± 0.04	1838.66 ± 0.04
Decay products	stable	$e^{\pm} + \nu + \nu$	$\mu^{+} + \nu$	$\mu^{-} + \nu$	$\gamma + \gamma$		$p + e^{-} + \nu$
Mean life		$2.22 \pm 0.2\ 10^{-6}$ sec.	$2.53 \pm 0.10\ 10^{-8}$ sec.	$2.44 \pm 0.18\ 10^{-8}$ sec.	$5\ 10^{-15}$ sec.		12.8 ± 2.5 min.
Spin	$\frac{1}{2}$	$\frac{1}{2}$	0	0	0	$\frac{1}{2}$	$\frac{1}{2}$
Parity			(-)	(-)	(-)		

TABLE II

Pion kinetic energy	$p\tau/\mu$
5 MeV	2.06 10^2 cm
10	2.95
15	3.66
20	4.26
25	4.77
30	5.27
35	5.79
40	6.19

* * *

TABLE III

The incident meson spectrum

Incident energy (MeV)	Decays measured	Measured path length = 1 cm.	Measured path length = x gr/cm^2	Corrections		Corrected path length gr/cm.^{2}
				Projection = α_p (%)	Coulomb scatt. = α_c	
5 - 10	465	1.20×10^5	317	6	6	388
10 - 15	601	1.98	522	8	3	657
15 - 20	655	2.58	677	10	2	896
20 - 25	559	2.51	659	12	1.5	900
25 - 30	262	1.32	348	13.5	1	486
30 - 35	215	1.20	312	15.5	1	447
35 - 40	84	0.50	132	17	0.5	192
Total (10-35)	2292	$9.59\ 10^5$	2518			3386

$$\text{Corrected path length} = \frac{\times}{1-\alpha_p + \alpha_c} \times \frac{100}{82}$$

* * *

TABLE IV

Accepted $^{+}$-p scattering events

Incident energy (MeV)	scattering angle c. of m. system (degrees)
10 - 12	152
16	74
19	110
21	137
23	150
23	157
25	116
26	152
26	79
25 - 27	78
25 - 27	80
29	114
31	141
32	70
31 - 34	165

*

* *

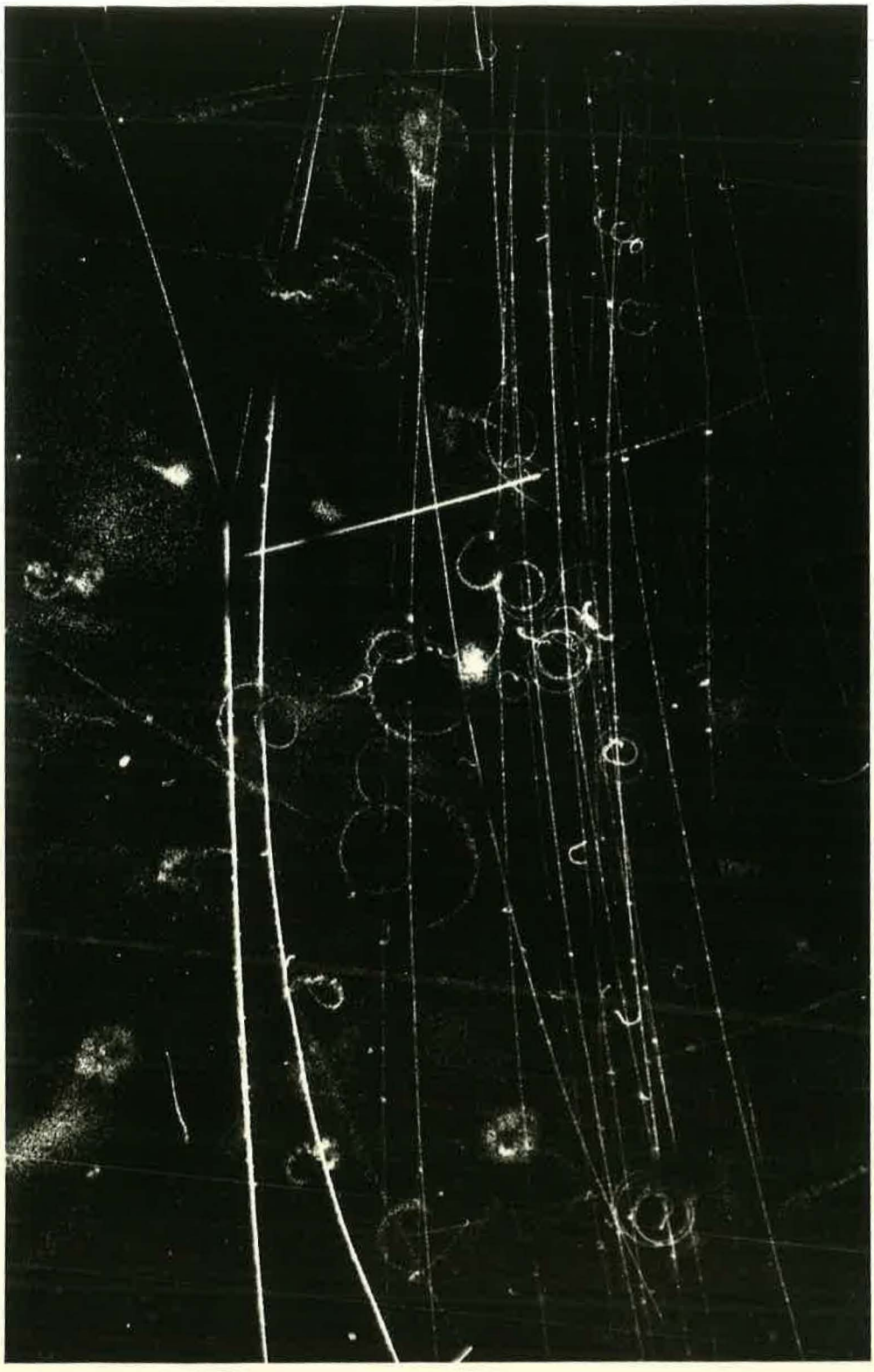

References

1) For a summary see R.E. Marshak - Mesons Physics, Mc Graw Hill Book Company 1952.
H.A. Bethe, F. de Hoffmann, S.S. Schweber - Mesons and Fields vol. 1 and H.A. Bethe, F. de Hoffmann - Mesons and Fields, vol. 2 - Row Peterson New York 1955.

2) H. Yukawa Proc. Phys. Math. Soc. Japan 17, 48, 1935.

3) a. ref. 1) and

b. E.M. Henley, M.A. Rudermann, J.L. Steinberger - Annual Review of Nuclear Science, Annual Reviews - Stanford 1953.

c. M. Gell-Mann & K.M. Watson, Annual Review of Nuclear Science - vol. 4, Annual Reviews - Stanford 1957.

d. R.H. Dalitz - Progress in Nuclear Physics, 4, Pergamon Press. London 1955.

4) G.C. Wick - Review of Mod. Physics, 27, 339, 1955

5) a. M. Gell-Mann, M.L. Goldberger, W.E. Thirring - Physics Review 95, 1612, 1954.

b. A. Salom - Nuovo Cimento 3, 424, 1956.

6) a. R. Krønig, J. Opt. Soc. Am. 12, 547, 1926.

b. H.A. Kramers - Atti Congr. Int. Como 2, 545, 1927.

7) L.I. Shiff - Quantum mechonics - Mc Graw Hill Book Company, New York 1949.

8) J.M. Blatt & W.F. Weisskopf - Theoretical Nuclear Physics - John Wiley and Sons, New York 1952.

9) E. Fermi - Suppl. Nuovo Cimento 1, 17, 1955.

10) N.F. Mott and H.S.W. Massey - The Theory of Atomic Collisions, The Clarendon Press. Oxford 1949.

11) W. Heisenberg - Z. Phys. 17, 1, 1932.

12) F. Solmitz - Phys. Rev. 94, 1799, 1954.

13) L. van Hove - Phys. Rev. 88, 1358, 1952.

14) H.L. Anderson, E. Fermi, R. Martin, D.E. Nagle - Phys. Rev. 91, 155, 1953.

15) J. Orear - Phys. Rev. 96, 179, 1954.

16) J. Orear - Phys. Rev. 100, 288, 1955.

17) a. Proceedings of the Third Rochester Conference on high energy nuclear Physics - Interscience Publishers, New York 1952.

b. Proceedings of the Fourth Rochester Conference on high energy nuclear Physics - Interscience Publishers, New York 1954.

c. Proceedings of the Fifth Rochester Conference on high energy nuclear Physics. Interscience Publishers, New York 1955.

d. Proceedings of the Sixth Rochester Conference on high energy nuclear Physics. Interscience Publishers, New York 1956.

18) R. Jastrow - Phys. Rev. 81, 1165, 1951.

19) R.E. Marshak - Phys. Rev. 88, 1208, 1952.

20) H.P. Noyes & A.E. Woodruff - Phys. Rev. 94, 1401, 1954.

21) H.L. Anderson & E. Fermi - Phys. Rev. 86, 794, 1952.

22) G. Bernardini & E.L. Goldwasser - Phys, Rev. 95, 857, 1954.

23) M. Benevento, G. Bernardini, D. Carlson-Lee, G. Stoppini, L. Tan - Nuovo Cimento 2, 344, 1956.

24) W.K.H. Panofsky, L. Aamodt, J. Hadley - Phys. Rev. 81, 565.

25) J.M. Cassels, G. Fidecaro, A.M. Wetherell, J.R. Wormald - Private communication.

26) J.A. Kuhner, A.W. Merrison, S. Tomabene - Private communication.

27) H.P. Noyes - Phys. Rev. 101, 320, 1956.

28) A. Roberts & J. Tinlot - Phys. Rev. 90, 951, 1953.

29) A. Roberts & J. Tinlot - Phys. Rev. 95, 137, 1954.

30) a. C.E. Angell & J.P. Perry - Phys. Rev. 91, 1283, 1953.

b. C.E. Angell & J.P. Perry - Phys. Rev. 92, 835, 1953.

c. S.W. Barnes, C.E. Angell, J.P. Perry, D. Millor, J. Ring, D. Nelson - Phys. Rev. 92, 1327, 1953.

31) S.L. Leonard & D.H. Stork - Phys. Rev. 93, 568, 1954.

32) J. Spry - Phys. Rev. 95, 1295, 1954.

33) J. Orear, W. Slater, J.J. Lord, S.L. Eilenberg & A.B. Weaver - Phys. Rev. 96, 174, 1954.

34) M.C. Rinehart, K.C. Rogers, L.M. Ledermann - Phys. Rev. 100, 883, 1955.

35) J. Orear - Phys. Rev. 98, 239, 1955.

36) S. Wheastone & D. Stork - Phys. Rev. 102, 251, 1956.

37) S.W. Barnes (See 17) d.)

38) A.M. Sachs, H. Winick and B.A. Wooten - Phys. Rev. 100, 1255, 1955.

39) D.E. Nagle, R.H. Hildebrand, R.G. Plano - R.S. I 27, 283, 1956.

40) M. Camac, A.D. Mc Guire, J.B. Platt & H.J. Schulte - Phys. Rev. 99, 897, 1955.

41) M. Stearns, M.B. Stearns, S. Debenedetti & L. Leipuner - Phys. Rev. 97, 240, 1955.

42) M.H. Alston, A.W. Crew, G. von Gierke, W.H. Evans - Mesons production in p.p. collisions to be published in "Proc. Phys. Soc."

43) M.H. Alston - Ph. D. - Thesis, University of Liverpool.

44) S.W. Barnes, D.L. Clark, J.P. Perry and C.E. Angell. - Phys. Rev. 87, 669, 1952.

45) J.J. Lord, A.B. Weaver, J. Orear - Phys. Rev. 93, 575, 1954.

46) R. Sagane, W. Derdziak - Phys. Rev. 92, 212, 1953.

47) E. Segré - Experimental Nuclear Physics, vol. 1 John Wiley & Sons N.Y. 1953

48) E.C. Fowler, W.B. Fowler, R.P. Schute, A.M. Thorndike & W.L. Wittemore - Phys. Rev. 91, 135, 1953.

49) R. Hofstadter & R.W. Mc Allister - Phys. Rev. 98 - 217 - 1955